Review Article

BIOMEDICAL Journal of Scientific & Technical Research

ISSN: 2574 -1241

DOI: 10.26717/BJSTR.2026.64.010038

Emerging Advances in Hemostatic Application of Biopolymeric Bionanocomposites

Chinonso Paul Agbata, Christopher Igwe Idumah*, Uchenna Allen Uzoukwu and Daniel Chibuzor Ekweonu

Department of Polymer Engineering, Faculty of Engineering, Nnamdi Azikiwe, Nigeria

***Corresponding author:** Christopher Igwe Idumah, Department of Polymer Engineering, Faculty of Engineering, Nnamdi Azikiwe, Nigeria

ARTICLE INFO

Received: October 19, 2025

Published: January 09, 2026

Citation: Chinonso Paul Agbata, Christopher Igwe Idumah, Uchenna Allen Uzoukwu and Daniel Chibuzor Ekweonu. Emerging Advances in Hemostatic Application of Biopolymeric Bionanocomposites. Biomed J Sci & Tech Res 64(3)-2026. BJSTR. MS.ID.010038.

ABSTRACT

A major cause of death arising from traumatic injuries in civilian and military segments is hemorrhage or hemostatic, wherein a notable degree of demise and complexities take place prior to paramedic involvement and hospital intervention. Therefore, it has become imperative to fabricate hemostatic materials capable of being applied via simplified steps to enable bleeding control through inducement of fast hemostasis, un-invasively, prior to reception of essential medical care by individuals. This paper elucidates emerging advancements in synthesization and construction of biodegradable hemostatic nanomaterials as well as bionanocomposites. The assemblage manipulation and fine-tuning of absorbable and degradable composition of hemostatic supramolecular architectures and nanoarchitectures have facilitated the fabrication of smart scaffolds and gadgets with capability of effective bleeding control thereby minimizing surgical and hospitalization time-frame. Therefore, this paper presents recently emerging advancements in biopolymeric bionanocomposites containing bioactive nanostructures for effective hemorrhage and hemostatic control and effect of interfaces.

Keywords: Hemostasis; Bioactive Nano-Constructs; Biopolymers; Biopolymeric bionanocomposites

Abbreviations: PEG: Polyethylene Glycol; PCL: Polycaprolactan; BSA: Bovine Serum Albumin; CS: Chitosan; MBG: Mesoporous Bioactive Glass; CS-SEP: Chitosan-Sepiolite; LCGH: Lupeol Embedded Chitosan-Gelatin Hydrogel; CLX: Chlorhexidine; PVP: Polyvinylpyrrolidone; MCs: Microcomposites; LGIB: Lower Gastro Intestinal Bleeding; HNTs: Halloysite Nanotubes; L-ECM: Liver Extracellular Matrix; KE-NPs: Keratin–Catechin Nanoparticulates; CCNa: Carboxymethyl Cellulose; HEC: Hydroxyethyl Cellulose; PVA: Polyvinyl Alcohol; PVPEM: PVP Electrospun Membranes; TAT: Thrombin-Antithrombin; RBCs: Red Blood Cells; AM: Acrylamide; EGCG: Epigallocatechin-3-Gallate; TXA: Tranexamic Acid; aPDT: Antibacterial Photo-Dynamic Therapy; ROS: Reactive Oxygen Species

Introduction

The interest in extorting differing synthetic techniques and macromolecular assemblage in fabricating effective hemostatic biopolymeric bionanocomposites possessing degradable backbones has recently escalated with the aim of effectively controlling their physicochemical features for attainment of the capability of interacting with blood constituents for rapid and effective hemostasis. A vast range of biopolymeric matrices/scaffolds/encapsulates including chitosan, polyethylene glycol (PEG), gelatin, PLGA, collagen, polycaprolactan (PCL), and so on, have been embedded with differing bioactive species/hemostatic agents (calcium, tranexamic acid, antibiotic agents (gentamicin, vancomycin, minocycline,etc.)), and/or nanoparticulates (silver, zinc, molybdenum disulfide, titanium dioxide, etc), as well as other natural products including cabreuva, turmeric and clove essential oils, and so on, to construct superior biopolymeric composites and bionanocomposites for effective hemorrhage, hemostatic control and wound mending [1-5]. Nanotechnological exploration has demonstrated capability of transforming and utilizing the microstructure on a nanometric level, to bequeath nanomaterials exhibiting veritable features including enhanced diffusivity and solubility, ease of penetrating physiologically affiliating barricades, broad specific surfacial area, gradual controlling, and specific releasing of drugs [6,7].

Asides the chemical constitution of hemostatic materials, other critical parameters includes size, dimension and morphology [8]. Recently, in depth studies has been conducted on nano-hemostatic nanomaterials including nanoparticles, nanosheets, liposomes, and self-assemblage nano-peptides, which offer greater leverage for the development of hemostatic materials [9,10]. Nanoparticles are col-

loidal particulates constituting of macromolecular substrates with a solid particulate dimension in range of 10–1000 nm. Here, charged nanoparticulates are capable of releasing electrostatic effects on blood cells or fibrinogens possessing opposite charges, and neutralize the surfacial charges, initiate its agglomeration, while promoting blood coagulation [11]. The blood is a veritable medium for assisting nanoparticulates in attaining specific tissues and organs possessing peculiar flow features, affecting platelets and nanoparticulates distribution within the vascular system [12]. Nanocomposite hydrogels are elevatable molecular polymeric matrices possessing a three-dimensional (3-D) network architecture capable of absorbing broad levels of water or biologically affiliated fluids [13].

Recently, nanocomposite hydrogels have become novel form of biomaterials because of enhancement of shear thinning features [14]. Inherent features of hydrogels are capable of enhancement through inclusion of differing nanomaterials as nano-reinforcements within the soft polymeric matrices, garnering nanocomposite hydrogels exhibiting enhanced features [15]. Hydrogel nanocomposites are made up of elevated hydrophilicity, high water absorption, flexibility, broad specific surface area as well as high adsorption capacity. Hydrogel nanocomposites are capable of concentrating blood cells and platelets, thereby facilitating bleeding stoppage. Simultaneously, a gel-like film layer is formed on the wound surface thereby mending the wound [16]. Numerous acute injuries/wounds induce irregular wounds or intra-porous bleeding thereby hindering efficiency by preventing the thin films or sheets of hemostatic materials from deep penetration within the wound. On the other hand, hydrogel nanocomposites appear in powdery form thereby forming in situ gel, capable of being utilized for hemostasis in irregularly and deep wounds/injuries [17]. Nanoparticulates are capable of easy penetration of biological barricades, wherein the can penetrate circulatory systems, and cells through endocytically affiliated processes, such as pinocytosis, phagocytosis, and endocytosis [18].

Nanoparticulates induce variations in erythrocytes, affecting blood viscosity thereby functioning as hemostasis [19]. In a study, bovine serum albumin (BSA) and chitosan (CS) were encapsulated within mesoporous bioactive glass (MBG) nanoparticulates (MBG@BSA/CS), thereby activating physiologically affiliated coagulation routes [20]. Silver nanoparticulates (AgNPs) possessing antibacterial features and prospects for promoting platelet agglomeration are prevalently utilized hemostatically affiliated nano-medical materials, capable of inducing dosage based hemolysis [21]. Individual super thin films, known as nano-films or nano-sheets, are two dimensional (2-D) nanomaterials which has garnered great attention in nanotechnology sphere recently. Nanosheets possesses broad surface area/aspect ratio with elevated transparency and high flexibility. On application to wounds, platelets, blood cells, and coagulation parameters can be concentrated through rapid water absorption [22].

Hemostatic nanofibers, constructed via electrospinning, have extensively been utilized for the wound dressing preparation, and in fabricating scaffolds for tissue engineering as well as drug delivery applications [23]. Chitosan and gelatin are usually applied in nanofibers formation for antimicrobial and hemostatic applications [23,24]. Nano-constructions which have shown hemostatic pre-clinic effectiveness in animal models, and sharing degradability features and nano-assemblies presence within their constitutions are notable. Degradable/absorbable hemostatic nano-constructions are separated into nanoparticulates, nanofibers and nano-sponges [23-25]. Therefore, this paper elucidates recently emerging advancements in biopolymeric bionanocomposites containing bioactive nanostructures for effective hemorrhage and hemostatic control.

Mechanism and Bio-Absorption of Hemostatic Nanocomposites

Nanocomposites are multi-phased solid nanomaterials composed of varying phases wherein at least a single phase has one dimension in the nanometric range [26]. Nanometric materials display notable prospects as effective hemostatic entities. Studies have revealed novel knowledge of the interactivities between materials and coagulation components at the nanometric level, thereby revealing critical properties of nanomaterials in blood coagulation including nanofibers aspect ratio, nanoparticles and nanofibers diameter, and the pore-architectures of nano-porous materials as elucidated in Figure 1 [27]. Differing nanomaterials are embedded during fabrication of hemostatic biopolymeric bionanocomposites including nanofibers and nanoparticulates [28,29]. Numerous hemostatic agents have been embedded within biopolymeric bionanostructures with demonstration of highly efficient hemostatic acumen. These hemostatic agents have differing mechanisms of operations, whereby for instance, chitosan, a naturally occurring positively charged polysaccharide, undergo interaction with the negatively charged thrombocytes and erythrocytes thereby facilitating adherence at the bleeding sites, thus aiding platelet agglomeration, hence, resulting in the creation of blood clots [30].

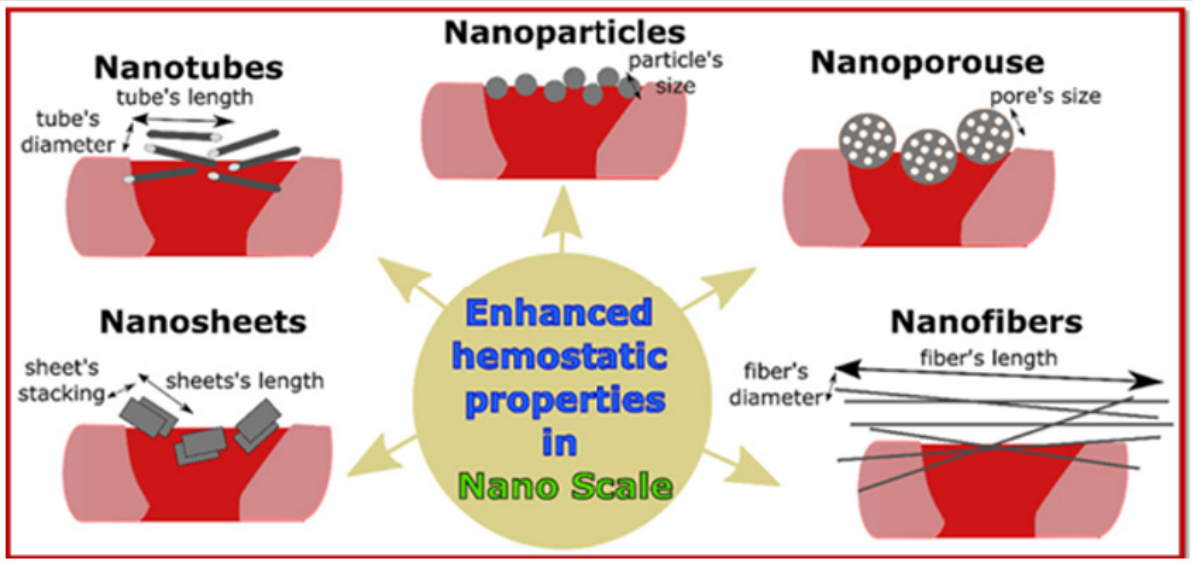

Figure 1: Nanometric features of different hemostatic agents [27].

Nanoclay Embedded Biopolymeric Bionanocomposites for Hemostatic Application

Nanoclay oriented hemostatic substrates have garnered great attention recently, even with reportage of hemostatic nanocomposite films composed of naturally occurring mixed-dimensional nanoclay constituting of naturally occurring 1-D and 2-D nanoclay minerals [31-34]. In a study, a series of chitosan-sepiolite (CS-SEP) nanocomposites films were constructed via conventional solution casting technique [31]. Here, sepiolite inclusion greatly incremented WVTR, folding propensity, porosity, and blood clotting abilities of the garnered bionanoarchitectures. Additionally, CS-SEP nanocomposite films demonstrated enhanced antibacterial abilities when compared with chitosan against gram positive (B. subtilis) and gram negative bacteria (*E. coli*). Furthermore, cytotoxicity assay revealed that the constructed nanocomposite film (CS7SEP3) displayed enhanced cell viability and cell proliferation rate against L929 mouse fibroblast cells in comparison with CS and hence, the constructed nanocomposite films can be utilized as a potential substrate for wound management. In another work, Lupeol embedded chitosan-gelatin hydrogel (LCGH) films were constructed via solution cast technique through chitosan and gelatin solution blending and with glycerol acting as plasticizer, subsequented by cross-linking with glutaraldehyde [32].

Antioxidant assay affirmed that lupeol and LCGH film demonstrated outstanding antioxidant features through the scavenging of both radicals at steadily incrementing rate which increased with time because of steady lupeol releasing. The MTT assay exposed that the CGH film obviously provided satisfactory cell viability and nil-toxicity demonstrating that chitosan/gelatin hydrogel film is a good delivery structure for sustained releasing of lupeol and LCGH films for improved wound mending [32]. In a similar work, chitosan/montmorillonite bionanocomposite films constituting of Chlorhexidine (CLX), with capability of offering extended CLX releasing were constructed with investigation of the antimicrobial, antibiofilm and cytotoxicity activities [33]. CLX was subjected to intercalation between the montmorillonite (MONT-Na) layers. Results reveal that all constructed films displayed good anti-microbial and anti-biofilm activities. Relative to cytotoxicity, the film constituting of MONT-CLX at 1% CLX inclusion resulted in zero cytotoxic thereby confirming the prospective usage of chitosan films containing MONT-CLX as prospective wound dressing substrate in hindering microbial wounds colonization [33]. In another investigation, elevatedly performing hemostatic nanocomposite films were constructed through the incorporation of naturally mingled dimensional palygorskite nanoclay enclosed with oxalic acid (O-MDPal) within chitosan/polyvinylpyrrolidone (CS/PVP) matrix.

Thus, Varying animals including snails and Chinese giant salamanders are capable of secreting mucus for moisturization, swelling and inflammation removal, and wound mending capability; depicting that these highly viscous bio-functionalized materials with inspiration from mucus are likely to demonstrate feasibility for biomedical usage. Thus, in a study, maltose-appearing injectable nanocomposites were developed via synergy of chitosan polysaccharide and clay rectorite for hemostatic application [35]. Attributable to the rectorite hemostatic features, the viscous nanocomposites decremented in vitro clotting duration by 43%. Furthermore, an in vitro porcine skin model affirmed that the viscous nanocomposite have stability for skin adherence while impeding blood bleeding successfully. Hence, these

viscous injectable nanocomposite films offer applicability as sustainable biomaterial for skin hemostasis [35]. The nanocomposite film demonstrated feasibility for wound mending usage [34]. The fabrication of effective, safe, ecobenign, and user-friendly hemostatic dressings is greatly challenging for researchers. A set of nanoclay minerals and plant extracts have attracted great attention attributable to their exceptional hemostatic efficiency and bio-safety.

Therefore, a facile solution casting technique has been utilized in fabricating nanocomposite films via inclusion of naturally occuring nanorod-appearing palygorskite (Pal) and herb-garnered hemostat dencichine (DC) originating on chitosan and polyvinylpyrrolidone. Significantly, the nanocomposite film displayed notable antibacterial efficiency and satisfactory cytocompatibility, in addition to in vitro wound mendability [36]. Summarily, Pal/DC synergized nanocomposite films display efficacy and suitability for wound repairing. The lower gastro intestinal bleeding (LGIB) duration of clotting can be minimized via simplified, cost-efficient, and naturally occurring halloysite nanotubes (HNTs). Hence, in a study study to minimize clotting duration through application of chitosan (CHT) and its microcomposites (MCs) constructed via a suspension emulsification approach with HNTs (CHT/HNTs MC). Furthermore, enhanced hemostatic and clotting features were CHT/HNTs MC1 > CHT/HNTs MC2 > CHT/HNTs MC3 > CHT > HNTs, respectively. Hence, it promoted the mitigation of bleeding disorders in LGIB with any antibacterial agents, especially ciprofloxacin [37]. During in dept nil-compressible wound mitigation, surgery, transplantation or post-surgical hemorrhage, rapid blood absorption and hemostasis are critical parameters considered to minimize unexpected demise from severe trauma.

Hence, in a study, a novel hemostatic biodegradable nanocomposite was constructed where decellularized liver extracellular matrix (L-ECM) was enclosed with two naturally occurring polymeric matrices (oxidized cellulose and chitosan) in association with thrombin [39]. Plant-garnered oxidized cellulose nanofiber (TOCN) and Chitosan (CS) from deacylated chitin were self-arranged with each other via electrostatic interactivities as depicted in Figure 2. ECM was constructed using whole tissue de-cellularization procedure and embedded within the bionanocomposite as a collagen source along with other integrated growth parameters for promotion of wound mending. Thrombin was additionally incorporated with the polymeric matrices via freeze drying for the material improved hemostatic efficiency [38]. Unmitigated bleeding is capable of resulting in critical injury and eventual death, occurring in some emergency scenarios. Previously, keratin has been depicted as good hemostatic substrate. Nevertheless, the hemostatic usage of pristine keratin materials is hindered by keratin's inferior physical features.

Thus, in a work, a hemostatic hydrogel was fabricated through the addition of keratin–catechin nanoparticulates (KE-NPs) within cellulose hydrogel. Keratin garnered from human hair was initially synergized with EGCG, the basic component of catechins, to attain the self-assemblage of nanoparticulates [39]. The fabricated KE-NPs possess a spherical geometry with a particulate dimension of around 40 nm. KE-NPs were subsequently embedded within cellulose hydrogel, resulting in cellulose/keratin–catechin bionanocomposite hydrogel (KEC). The garnered KEC displayed good adherence and hemadsorption, causing fast blood coagulation (Figure 3). Rat model study revealed that KEC displayed capability of restraining blood loss thereby serving as a novel hemostatic material [39]. A notable mechanism through which nanomaterials inhibit bleeding is via activation of platelets by mimicking platelet-activating parameters. Certain studies utilized this hemostasis technique in fabricating collagen mimetic peptides created by nanofibers for activating platelets thereby hindering bleeding [40]. Additionally, nanomaterials parameters including roughness are linked with platelet activation [41].

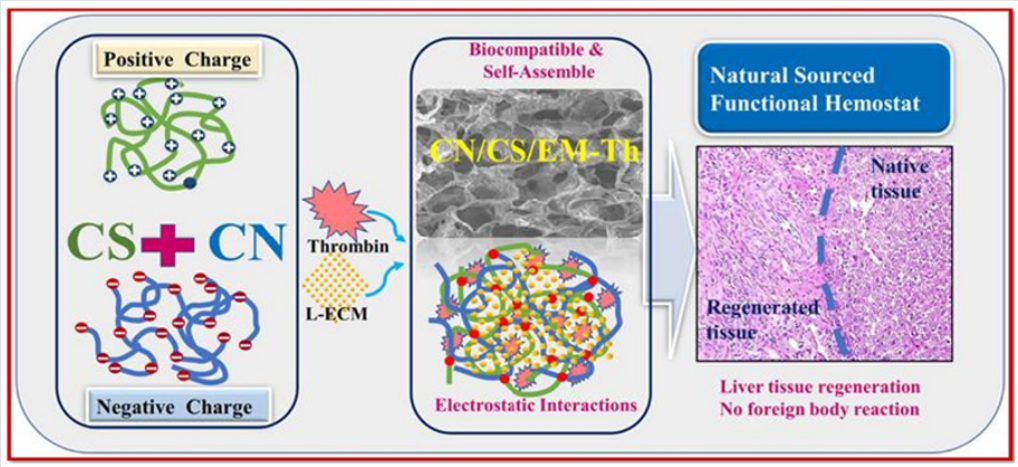

Figure 2: Elucidation of the features of synergized CS-TOCN bionanoarchitectures [39].

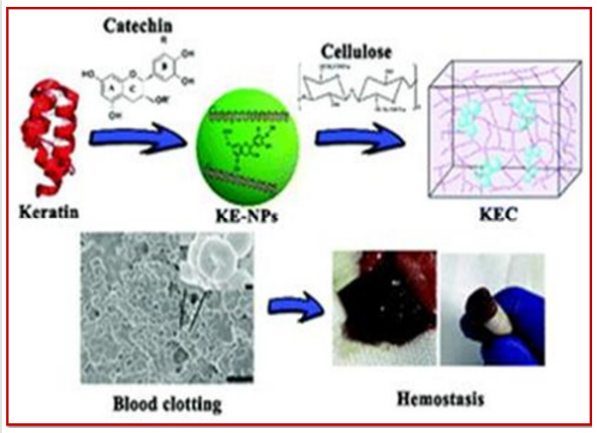

Figure 3: Mechanism of operation of TOCN/Chitosan bionanocomposite for hemostasis and wound mending [40].

Biodegradable Cellulose Bionanocomposite Hemostatic Nanomaterial

A new biodegradable cellulose-oriented composite hemostatic material was prepared by cross-linkage of sodium carboxymethyl cellulose (CCNa) and hydroxyethyl cellulose (HEC), subsequented by vacuum freeze-drying route [42]. The garnered cellulose composite material was neutral in pH and spongy possessing a density of 0.042 g/cm3, a porosity of 77.68%, and an average pore size of 13.45 μm. The composite's compressive and tensile strengths were 0.1 MPa and 15.2 MPa, respectively. Data garnered revealed that the new cellulose composite is potentially an implantable hemostatic material in clinical settings [42]. The cellulose hemostatic composite sponge fabricated in circular disk-configured molds was white, spongy, and pliable with good flexibility and slightly rough on the upper and lower surfaces (Figures 4(a) & 4(b)) [42]. Post 21 days of implantation, no residue visible appeared to the naked eye, hence variations in the materials are presented in Figure 5 [42]. Herein, the cellulose composite material exhibited a good hemostatic disposition with biocompatibility, and degradability. Furthermore, it also exhibited good physical and mechanical features, with further capability to be tuned by alteration of the ratio of the cellulosic polymeric or material architecture to better satisfy clinical requirements. Additionally, being an implantable biomaterial, the cellulose composite is capable of being optimized in drugs conveyance, like hemostatic entities and antitumor drugs, thereby playing double function in attaining both hemostasis and tumor dissemination for the future [42].

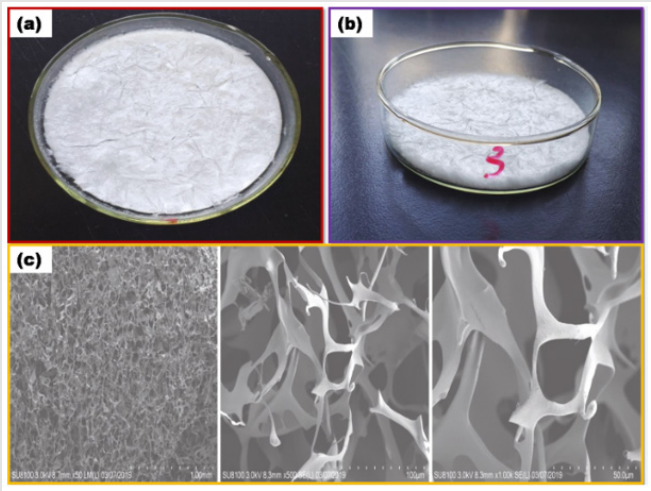

Figure 4:
a) Cellulose composite morphology,
b) A hemostatic degradable substrate.
c) SEM image of cellulose hemostatic composite substrate [43].

DOI: 10.26717/BJSTR.2026.64.010038

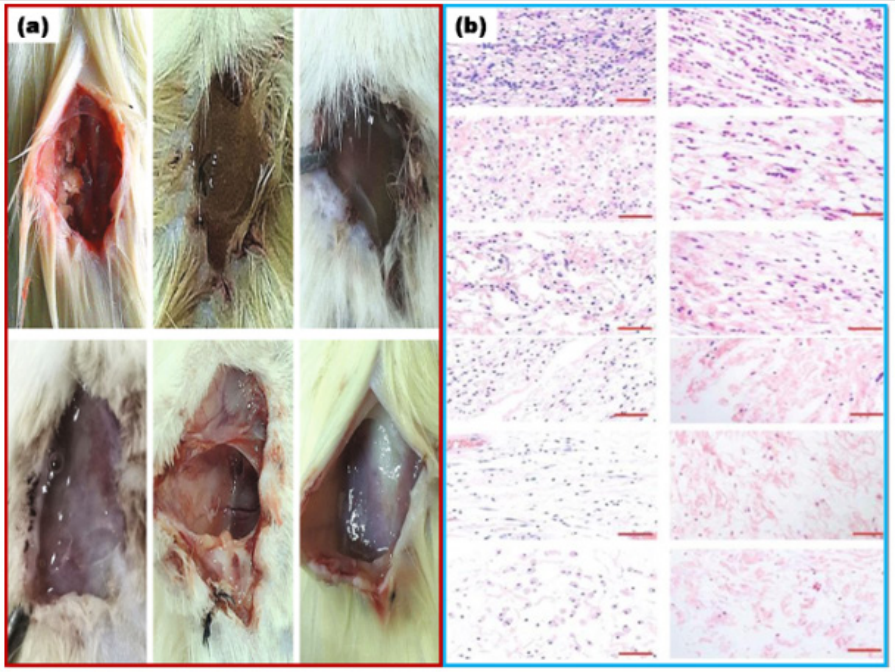

Figure 5:
a) Morphological variations in cellulose composite degradation in rats. Post degradation.
b) Histo-pathological observations revealed some inflammatory cellular infiltration in both implant and control groups (a-l) [43].

Porous Cellulose Based Fibrous Composite with Versatile Hemostatic Efficacy and Geometric Alignment for Hemorrhage: Herein, a self-broadening porous composites (CMCP) emanating from novel carboxymethyl cellulose (CMC) fibers and acetalized polyvinyl alcohol (PVA) was constructed for controlling lethal hemorrhage. The CMC fibers possessing even fibrous architecture, elevated absorption of liquid and pro-coagulating ability, were evenly distributed within the biopolymeric bionanocomposite matrix. The garnered composites exhibited unique fiber-porous architecture, outstanding absorption capacity, rapid liquid-powered self-expanding capacity and elevated fatigue inhibition, and physical-chemically, their performance displayed capability of fine-tuning via varying CMC composition (Figure 6) [43]. The CMC fibers constructing routh is presented in Figure 6a. Vital FTIR peaks are depicted in Figure 6b, while mechanical strength and adhesiveness relative to adherence to the glassware in the wet state are presented in Figure 6c. The micro-architecture of the CMC is observable in Figure 6d [43]. Post complete water absorbtion, the fibers are almost transparent revealing a certain strength, while absorbed water could not undergo seeping under pressure (Figure 7a).

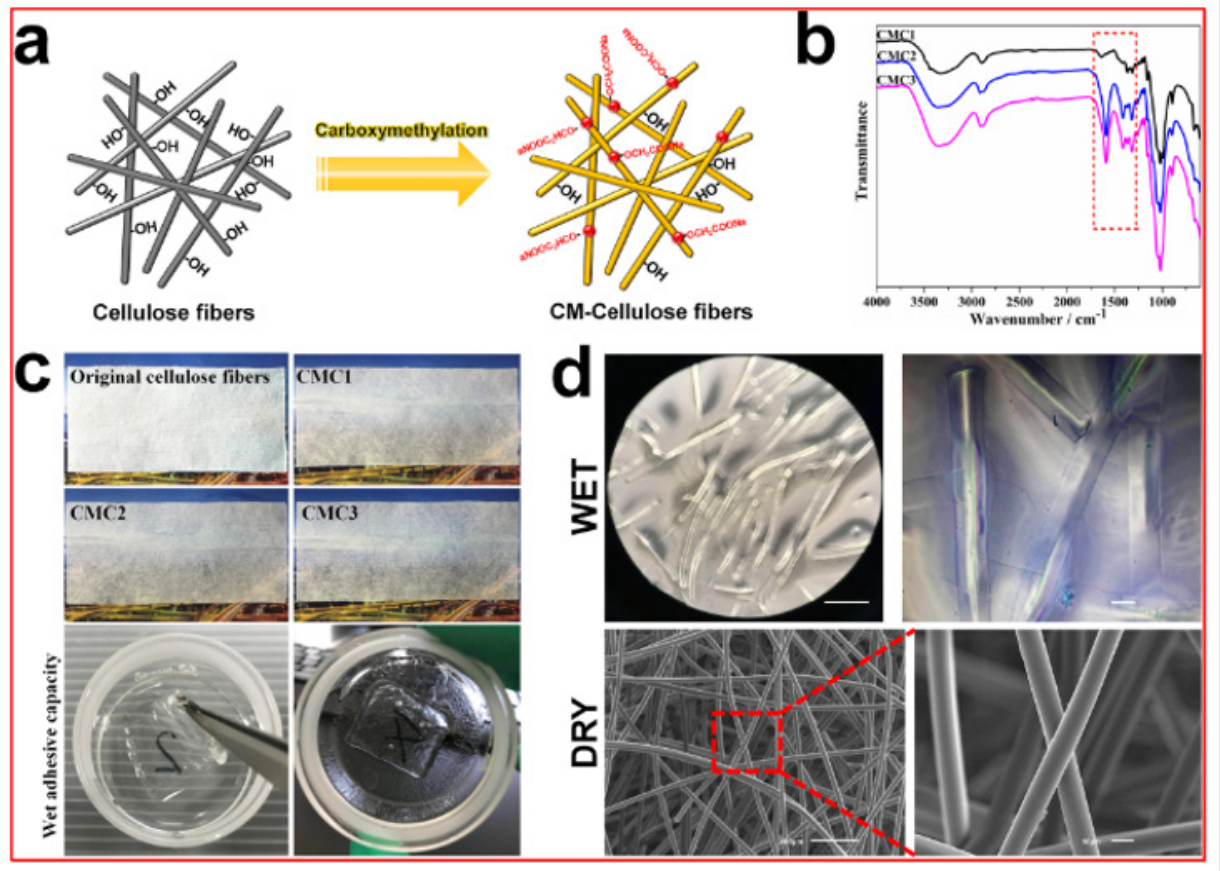

Figure 6:

a) CMC fibers fabrication.

b) FTIR spectra of varying CMC specimens.

c) Macroscopic observation of varying cellulose and CMC samples in wet state.

d) CMC micro-architecture in dry and wet state [44].

The treated fibers also displayed outstanding spinnability with capability of being spun into even fibrous cloths with elevatable deformability (Figure 7b) [43]. In vitro examination reveals that this porously composite display strong blood clotting propensity (Figure 8). CMCP composite morphology post and prior water absorption corresponding to self-expanding mechanism depicted in Figure 8d. The vast CMC fibers are observable within CMCP, both residing within the internal pores and interspersed within the polymeric matrix (Figure 8b), and CMC composition, whereas the pore size distribution gradually became uniform (Figure 8c). The schematic representation of CMCP absorbing water and undergoing self-expansion is presented in Figure 8d. The morphology of the CMCP composite before and after absorbing water corresponded with the self-expanding mechanism depicted in Figure 8d. CMCP composites exhibited higher cell biocompatibility with cell number higher in comparison with the control group on daily counting (Figure 9a).

DOI: 10.26717/BJSTR.2026.64.010038

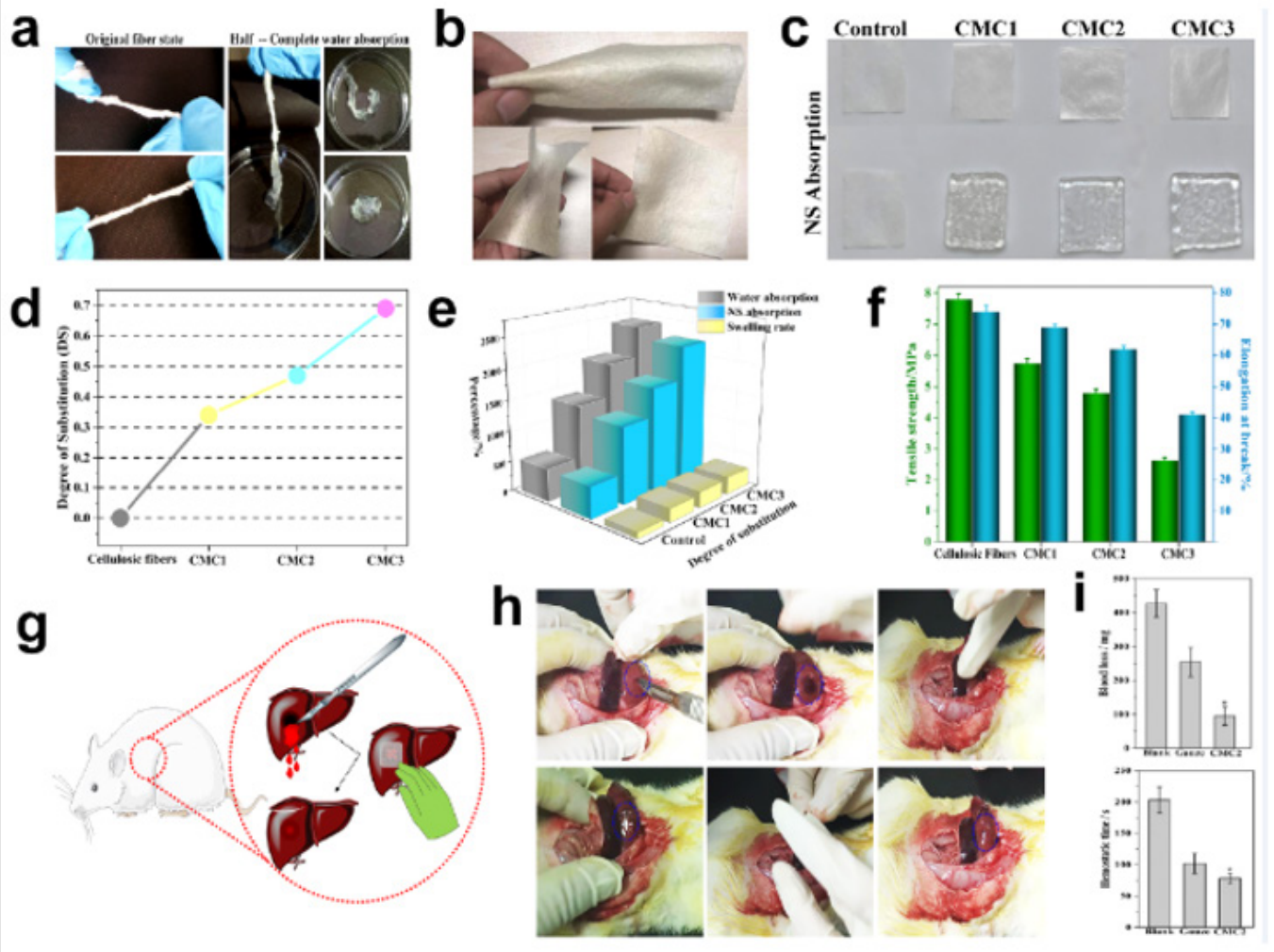

Figure 7:

a) CMC original architecture and the morphological variation during water absorption.
b) The CMC fibers are capable of being spun into fibrous cloth with outstanding flexibility.
c) Fibrous cellulose macroscopic images with differing CMC fibers prior and post absorbing normal saline.
d) The link between the DS of differing CMC specimens and the duration of reaction. The swelling ratio, adsorption capacity
e) And the mechanical strength and toughness
f) Of CMC with differing DS. Schematic representation
g) And macroscopic images
h) Of the in vivo hemostatic evaluation of the CMC2.
i) Blood releasing and hemostatic duration.

DOI: 10.26717/BJSTR.2026.64.010038

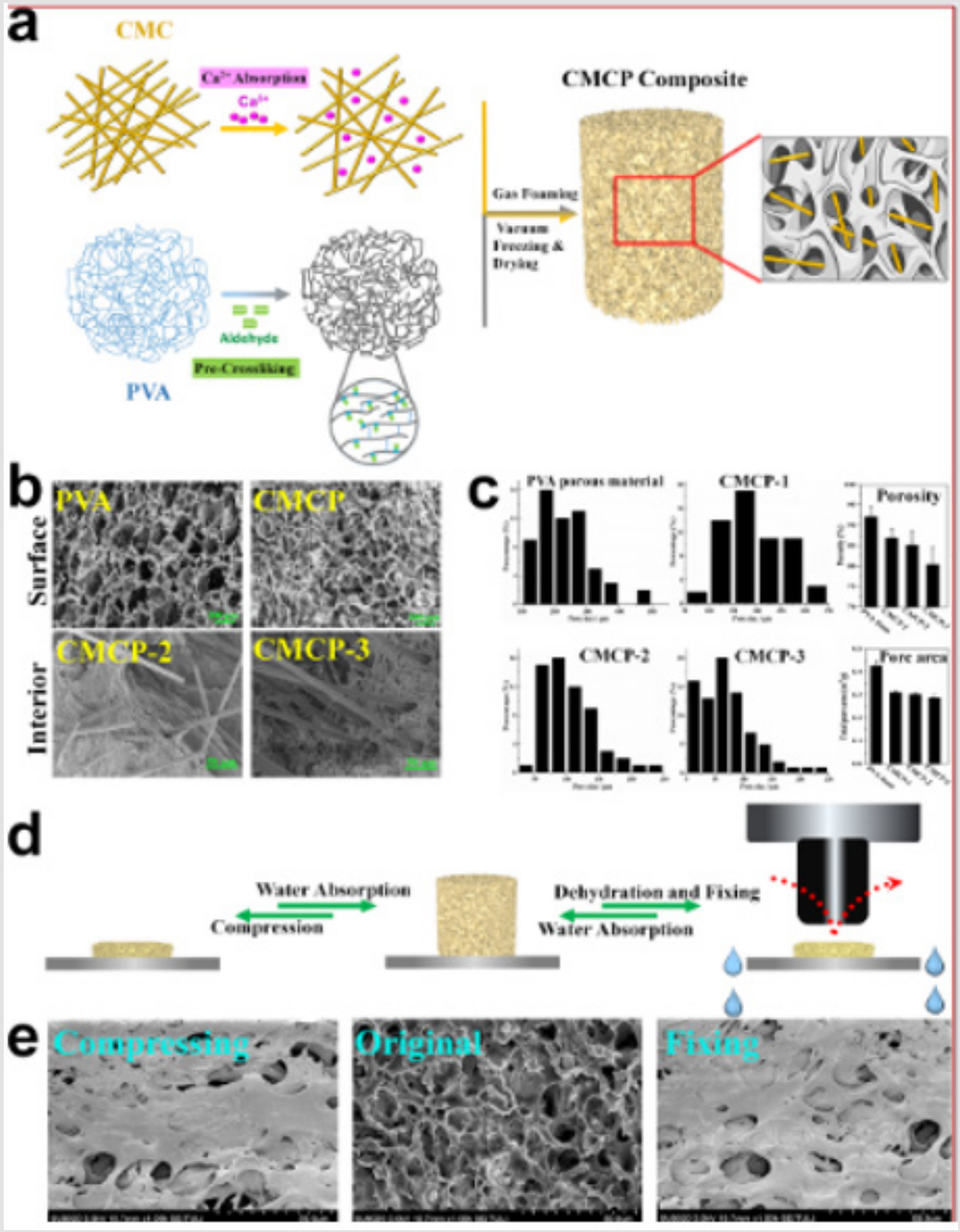

Figure 8:

a) Schematic elucidation of CMCP composites fabrication.
b) SEM images of porous PVA materials and CMCP composites.
c) Pore dimensional distribution, porosity and overall pore segment of differing materials.
d) Elucidation of the liquid-triggered self-expansive mechanism.
e) CMCP surfacial morphology in compressed state, original geometry and configuration-fixated state.

DOI: 10.26717/BJSTR.2026.64.010038

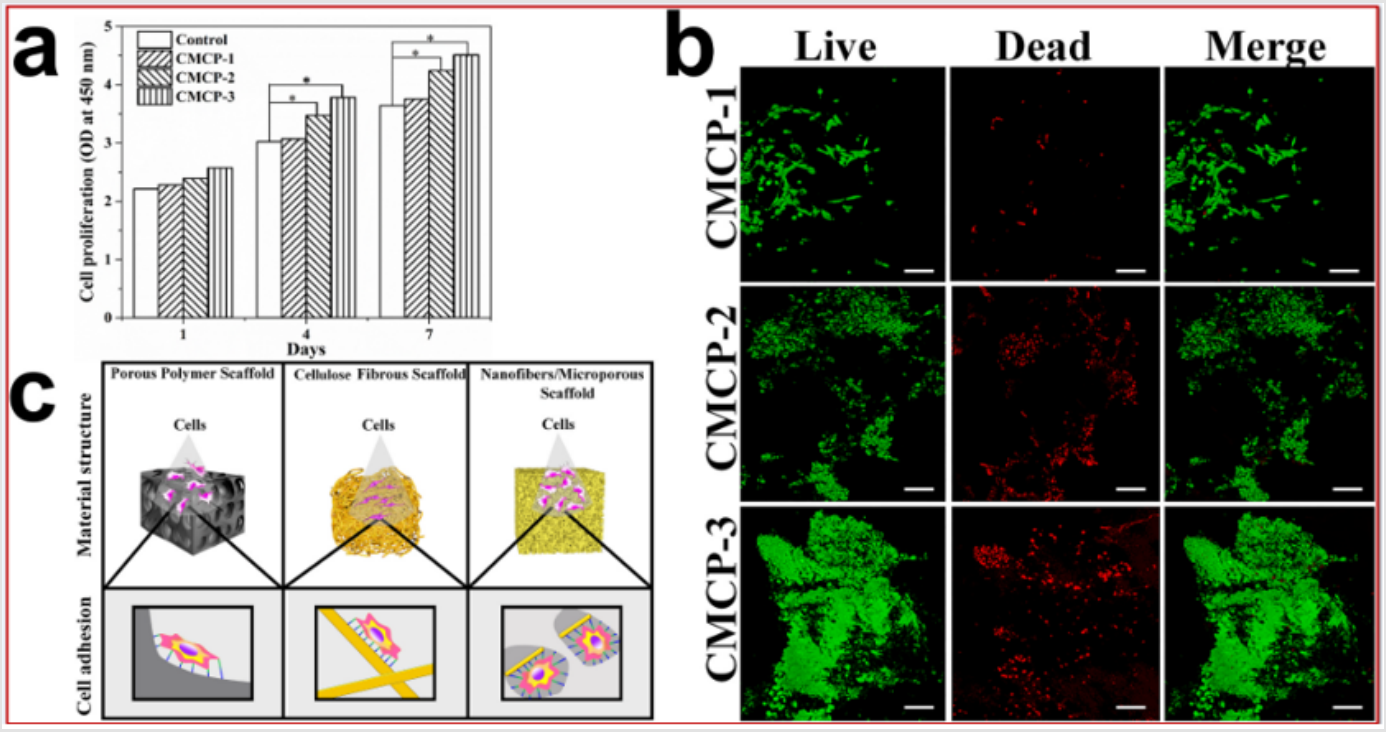

Figure 9:

a) CMCP composites cyto-toxicity with differing CMC composition.

b) Live-Dead staining of L929 cells seeded on the surface of differing composites post culturing for 7 days. Live cells emit green fluorescence, while dead cells emit red fluorescence. Scale bars: 100 μm.

c) Effects of differing material architectures on cell binding and spreading [44].

The water absorption affinity for CMCPs, mildly decremented with incrementing CMC composition, attributable to high compact fiber- interspersed porous network creation which delayed or hindered water from penetrating the composites (Figure 10a). Tensile stress-strain curves of the composites are exhibited in Figure 10b. Figure 10 (c-f) depicts notable fiber filling effects of CMC on CMCPs as well as the elevated composites compressive strength. The compression stress-strain curves of the materials post 50 cycles at the strain of respectively, are also depicted in Figure 10 (g–i) [44]. Figure 11 (a-f) depicts notable fiber reinforcing effects of CMC on CMCPs and elevated composites compressive strength. The compression stress-strain curves of the materials post 50 cycles at the strain of 40%, 60% and 80%, respectively, depicted in Figure 11 (g,h) [43]. Figure 12 reveal that varying mechanisms within CMCP acted synergistically to enhance hemostasis attributable to numerous activities.

DOI: 10.26717/BJSTR.2026.64.010038

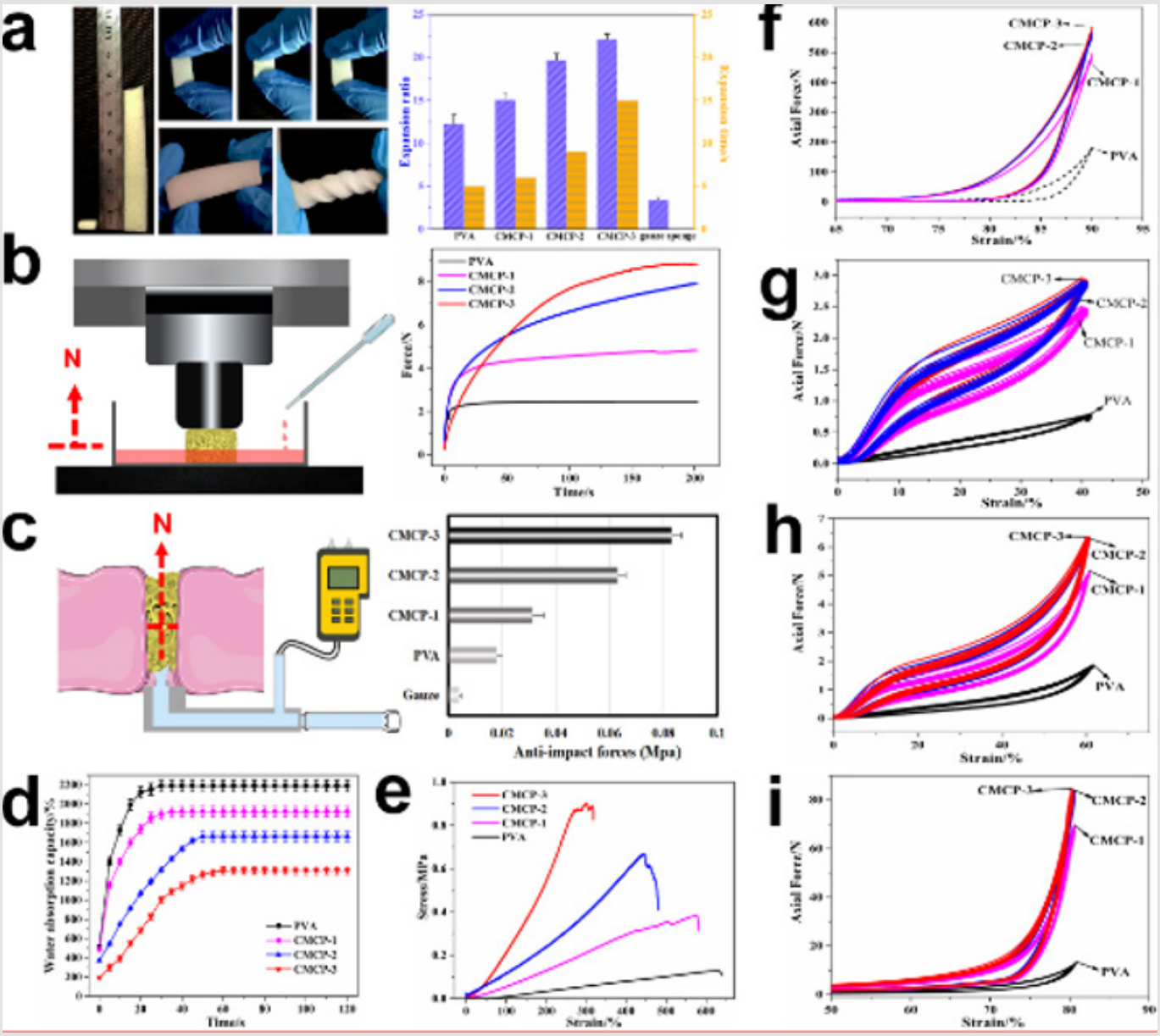

Figure 10:

a) CMCP composites possessing differing CMC content cytotoxicity (n = 3 per group).

b) Live-Dead staining of L929 cells situated on the surface of differing composites post 7 days culturing.

c) Impact of differing material architectures on cell binding and spreading [44].

DOI: 10.26717/BJSTR.2026.64.010038

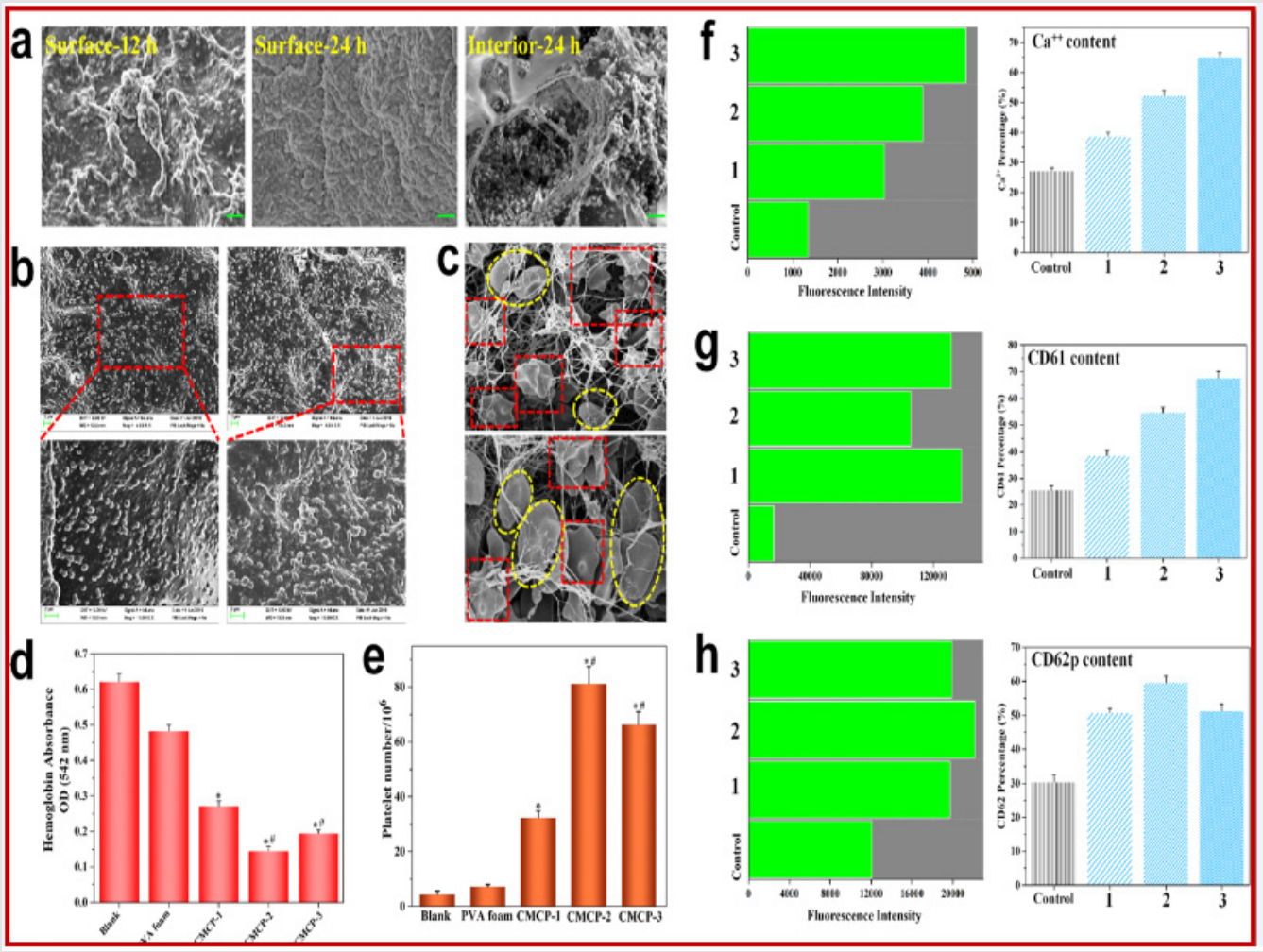

Figure 11:

a) CMCP macroscopically images prior and post liquid absorption, and the compression inhibiting capacity, flexibility, deformability and expansion disposition of CMCP in wet state.

b) Elucidation of dynamic expansion force test and variation in expansion forces of differing materials during progressive blood absorption.

c) Schematic elucidation of impact hindering examination and equivalent anti-impact stress of differing materials.

d) Water absorbing tendency and tensile features of differing materials.

e) Axial forces of differing composites on bearing of a 90% compression strain

f) and the cycling compressive curves (50 cycles) of differing composites with strains of 40%

g) 60%

h) And 80%

i) Respectively [44].

 DOI: 10.26717/BJSTR.2026.64.010038

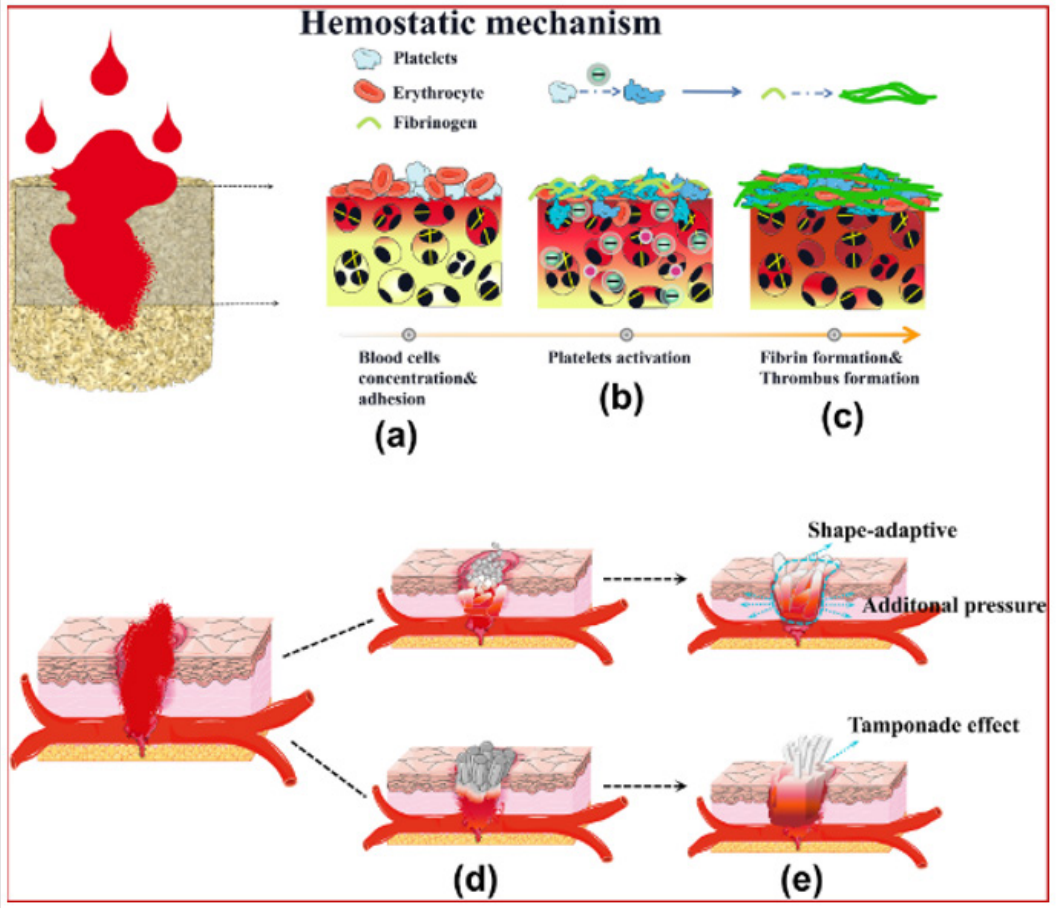

Figure 12: CMCP multiple mechanisms synergistically improve hemostasis.

a) CMCP quickly absorbed in blood, engulfed and concentrates blood cells by its fiber- interspersed porous network.

b) Adhered platelets and blood clotting parameters were activated by CMCP.

c) Rapid formation of stable thrombus.

d) CMCP samples were made into differing geometry for the arterial bleeding treatment.

e) CMCP absorbed blood and self-elongated, closed the wound via tamponade effect, imparted auxiliary pressure at enveloping tissues and vessels, and finally entirely took the configuration of the wound cavity via shape-adaptive capability to thereby attaining hemostasis [44].

Nanoclay-Polyvinylpyrrolidone (PVP) Membranes for Hemostatic Control: Hemostatic nanoclay nanoparticles can undergo connection by polymeric matrices to change nanoclay flour into nanoclay membranes for acute hemostasis. Some biomaterials fabricated involving nanoclays have functioned as efficient hemostats, including hydrogels such as gelatin/polyacrylamide (PAAm)/laponite hydrogels and sponges such as graphene (GN)-kaolinite or GN-montmorillonite composite sponge [44-47], depicted as strict and intricate modifications with elevated costs as medical hemostats. Hydrogels and sponges exhibit good shape memory but inferior mechanical strength attributable to their inherent inter-linked macro-porous architectures, and polymeric binders' fill-up and inhibit the nanoclay pores and layer gaps, inducing low clay utilization as active parts [48]. Electrostatic spinning is a prevalently utilized membrane synthesizing route which is capable of being embedded within nanoclays to facilitate easy fabrication of light, fluffy, and soft membrane substrates [49]. Herein, an efficient and fast nanoclay-oriented hemostatic membrane with nanoclay particulates embedded within polyvinylpyrrolidone (PVP) electrospun fibers was constructed [50].

The nanoclay electrospun membrane (NEM) with 60 wt% kaolinite (KEM1.5) demonstrated better and more rapid hemostatic disposition in vitro and in vivo with satisfactory biocompatibility compared with most other NEMs and nanoclay-oriented hemostats, gaining from its fertile hemostatic functioning sites, robust fluffy framework, and hydrophilic surface. The effective hemostatic bandages situated on nanoclay electrospun membrane are efficient potential hemostat material in practical application [50]. Fast efficient bandages situated on NEMs were fabricated by electrospinning with sheet-like kaolinite, tube-like halloysite and rod-like palygorskite (Figure 13a) [50]. The nanoclays were embedded with PVP electrospun membranes (PVPEM), including kaolinite EM (KEM1.5, 2.0, 2.4), halloysite EM (HEM1.5) and palygorskite EM (PEM1.5), respectively. The elevated flexibility (easily twisting 360° in situ) and of NEMs fabricability are garnered from the electrospun substrate (Figure 13b), positioning them appropriate for hemostatic uses. The SEM images (Figure 13c) revealed that kaolinite particulates with single sheet physical architectures were evenly and partially positioned on the KEM surface (the best architectures were garnered with a mass ratio of 1:1.5 (KEM1.5) [50].

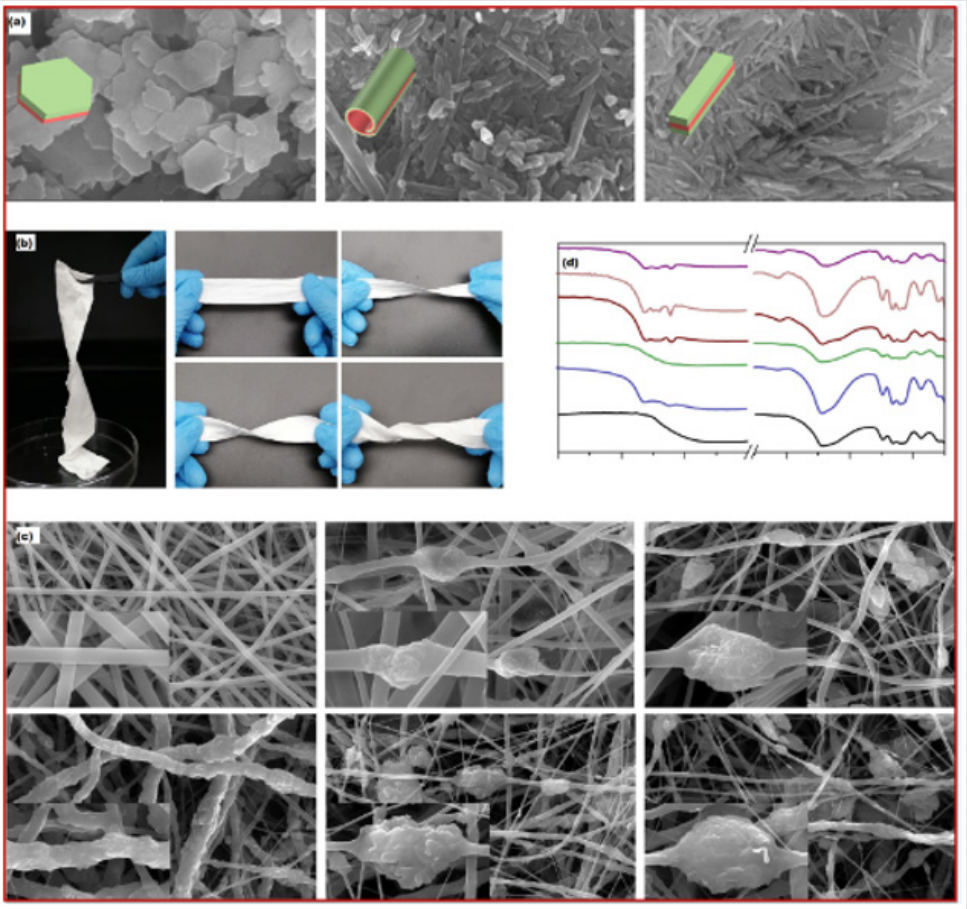

Figure 13: Construction, surfacial architecture and features of the nanoclay membranes.

a) SEM images of kaolinite, halloysite and palygorskite, respectively. Scale bar, 500 nm.

b) Photographic images of clay-membrane strips with differing extents of in situ twisting. Scale bar, 10 cm.

c) SEM images of PVPEM, HEM1.5, PEM1.5, KEM1.5, KEM2.0, and KEM2.4, respectively. Scale bar, 10 μm. The insets in (c) are the corresponding magnified SEM images. Scale bars in the insets of (c), 2 μm.

d) The localized magnified FT-IR spectra of PVPEM, HEM1.5, PEM1.5, KEM1.5, KEM2.0 and KEM2.4, respectively. Data were analyzed from at least three independently experiments in (a) and (c). Source data are provided as a Source Data file [51].

Nevertheless, bulkish agglomerates on KEM 2.0 and KEM 2.4 were ascribed to the over-high kaolinite particulate mass ratio, piecing the completely enclosed architecture and restraining its hemostatic effectiveness [50]. The coagulation prospects and clot integrity were studied via continual experimental study and assessment of the absorbance (optical density, OD) of the supernatant. The clot post NEM modification demonstrated a steady state (best: KEM1.5, almost no hemolysis) after 120 min, while the clot with PVPEM displayed gradual hemolysis, and almost all clot was terminally hemolytic (Figure 15c), depicting inferior coagulation ability in vitro devoid active parts [50]. Summarily, serially designable nanoclay-organic self facilitated membranes were developed, displaying prospects to be directly utilized as acute hemostasis bandages [50].

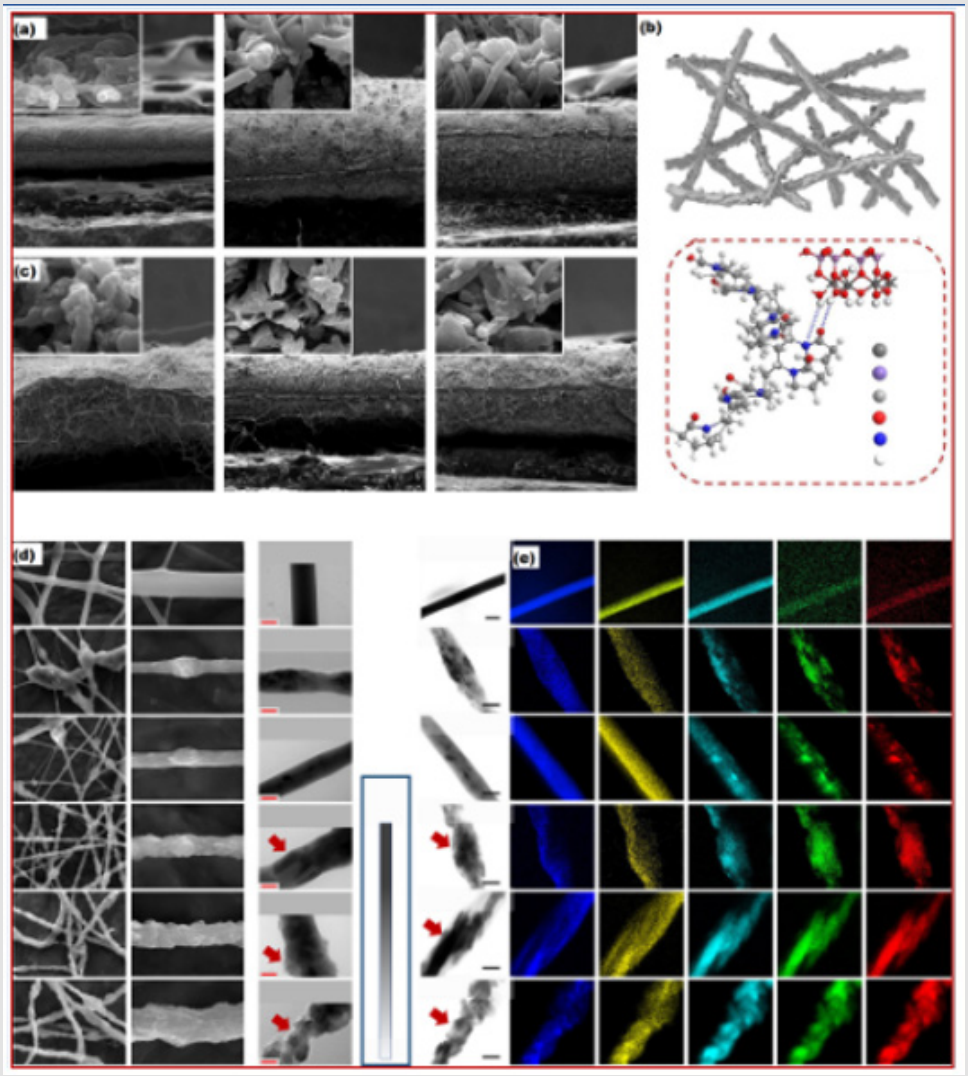

Figure 14: The interior architecture, interactivities and distribution attributes for nanoclay membranes.

a) Cross-section SEM images of PVPEM, HEM1.5, PEM1.5, KEM1.5, KEM2.0, and KEM2.4. Scale bar, 2 μm. The inset in (a) are the equivalent magnified SEM images of fiber section. Scale bars in the insets of (a), 2 μm.

b) The elucidation of the bonding interactivities between kaolinite and PVP.

c) The SEM images of individual sheet membranes (including the individual fiber in the inset),

d) TEM and

e) Mapping analysis images for PVPEM, HEM1.5, PEM1.5, KEM1.5, KEM2.0, and KEM2.4, respectively. Scale bars in (c–e) were 10 μm, 0.5 μm and 1 μm, respectively. Scale bars in the insets of (c), 2 μm. Data were analyzed from at least three independently experiments in (a) and (c–e). Source data are provided as a Source Data file [51].

DOI: 10.26717/BJSTR.2026.64.010038

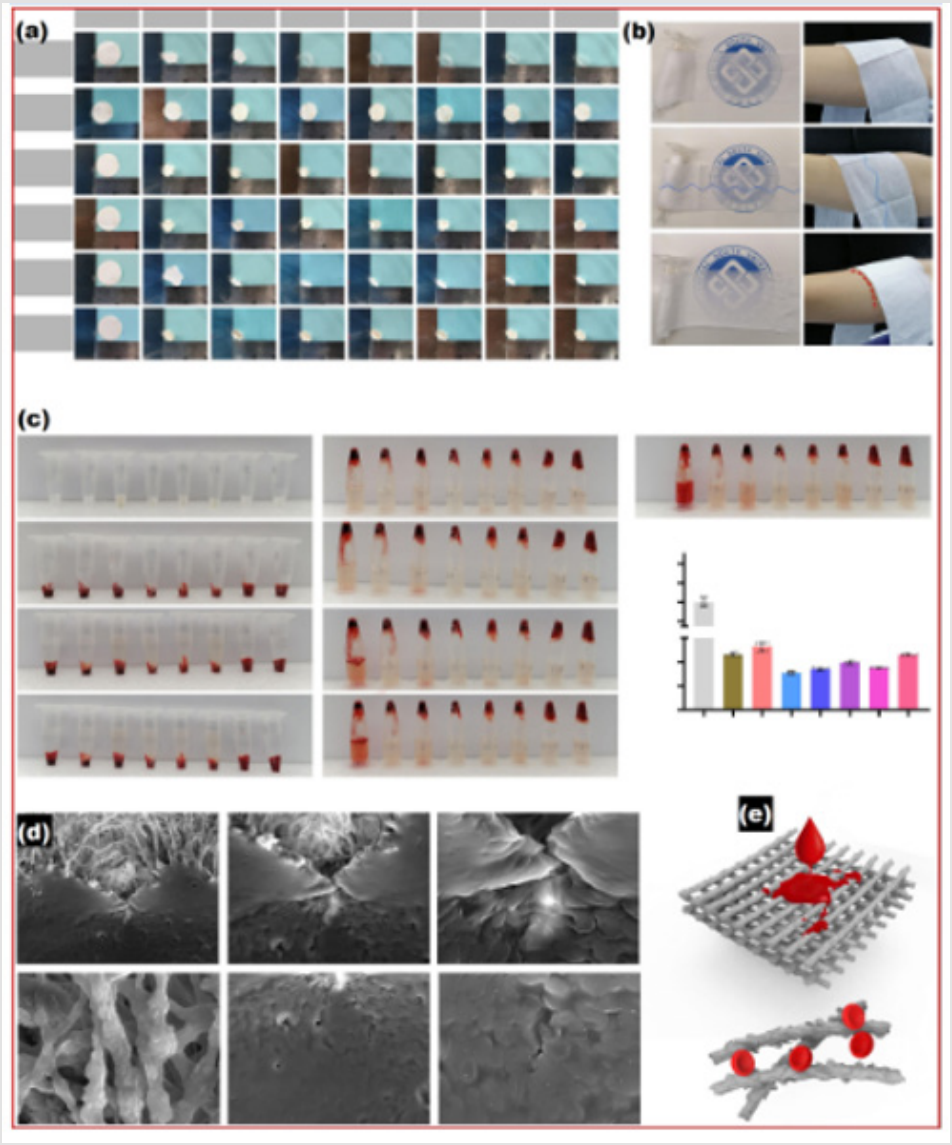

Figure 15: Shrinking and coagulating features of nanoclay electrospun membranes *in vitro.*

a) Specimen 7-day shrinking examination and results under the condition of steady temperature and humidity.
b) Photographic images of KEM1.5, ClG and CoG specimen for permeability and use on the skin.
c) Photographic images from the *in vitro* blood-clotting measurement and the corresponding relative OD values of the supernatant absorbance.
d) The SEM images of blood cells on the KEM1.5 surface.
e) Elucidation of blood parts permeation and contact to the KEM1.5 [51].

Fabrication of Cellulose Nanofibril/Casein-Situated 3-D Composite Hemostasis Scaffold for Prospective Wound-Mending Usage: Bleeding excessively in traumatic hemorrhage is main focus for naturally occurring wound mending and major reason for fatal trauma. The 3-D bio-printing of bio-inks gives required architectural complexity required for hemostasis process and specific cell proliferation in fast and controlled wound mending [51]. However, it is a challenge to fabricate appropriate bio-inks to construct specific 3-D scaffolds required for wound mending. Herein, a 3-D composite scaffold was constructed utilizing bio-printing technology and combined hemostasis system of cellulose nano-fibrils (TCNFs), chitosan, and casein in controlling blood-loss in traumatic hemorrhage (Scheme 1) [51]. Bio-inks consisting of casein bio-conjugated TCNF (composed of 104.5 ± 34.1 mg/g casein) utilizing the carbodiimide cross-linkage chemistry underwent subjection to bio-printing for customizable 3-D scaffold construction [51]. Furthermore, the 3-D scaffold composite underwent in situ cross-linkage utilizing a greenish ionic complexation route.

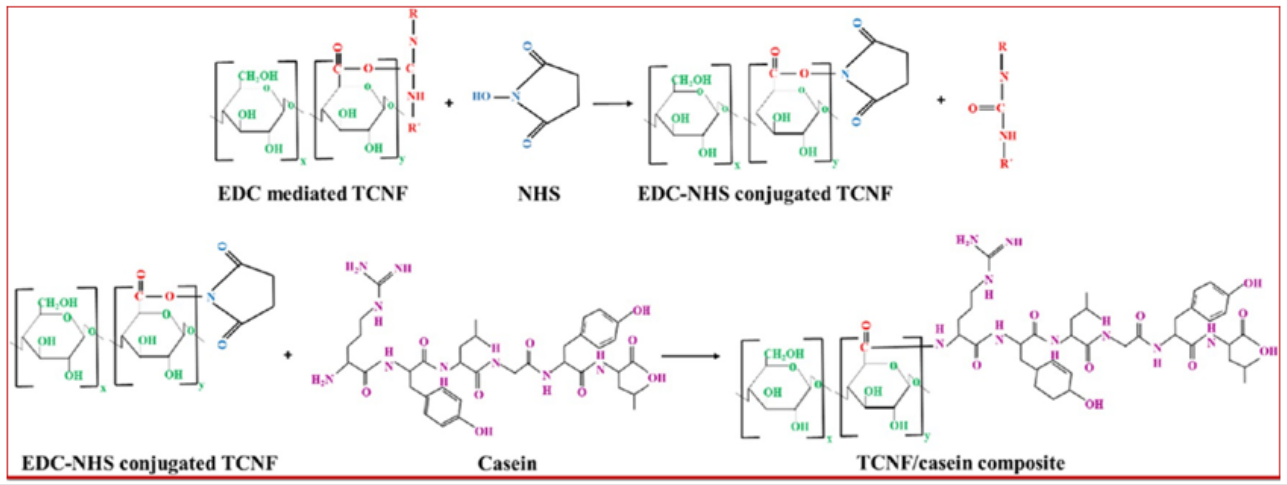

Scheme 1: **EDC/NHS-mitigated bio-conjugation reaction between TCNF and Casein [52].**

The covalent conjugation among TCNF, casein, and chitosan was affirmed using Fourier transform infrared (FTIR) spectroscopy, nuclear magnetic resonance (NMR), X-ray photoelectron spectroscopy (XPS), sodium dodecyl sulfatepolyacrylamide gel electrophoresis (SDS-PAGE), and X-ray diffraction (XRD) examination (Figure 16) [51]. The in vitro hemostasis prospects of the 3-D composite scaffold underwent examination via human thrombin-antithrombin (TAT) assay and adsorption of red blood cells (RBCs) and platelets. The 3-D composite scaffold displayed improved swelling disposition and rapid complete rate of blood clotting at individual duration compared with 3-D TCNF scaffold and commercial cellulose-situated dressings (Figure 17) [51]. Hence, in this study, an efficient concept for fabricating a 3-D composite scaffold from bio-printing of TCNF-situated bio-inks is capable of accelerating blood clotting and wound mending, demonstrating its prospective usage in minimizing blood loss during traumatic hemorrhage (Figure 18) [51]. In Figure 18a, TCNF TEM images exposed that the nano-fibrils varied in length, as they possessed even widths of 5–10 nm. Post casein bioconjugation to TCNF, the width of TCNF@casein conjugate nanofibril incremented to 15–20 nm with a few agglomerates, as observed in Figure 18b.

3-D composite scaffold's SEM images cross-section exposed notable fibrous structure alignment, as presented in Figure 18c–f. The architectural evaluation of the 3D scaffolds prior and post cross-linkage is demonstrated in Figure 18c–f [51]. In Figure 19, the SEM images expose adsorption. Broad RBC agglomerates and extended platelet pseudopods were seen on the surface of 3-D composite scaffold as observed in Figure 19 a-f [51]. The 3-D composite scaffold cytocompatibility underwent evaluation via 3-D cell culture routes in the presence of NIH 3T3 fibroblast cells for 72 h of incubation, as displayed by representative confocal images of cells in Figure 20. The in vitro cyto-compatibility examination is a notable attribute for any ECM mimicking matrix. The major objective of the cell-laden study was mimicking the cell survival on the 3-D composite scaffold and examines the cytotoxicity, which is paramount for wound mending [51].

DOI: 10.26717/BJSTR.2026.64.010038

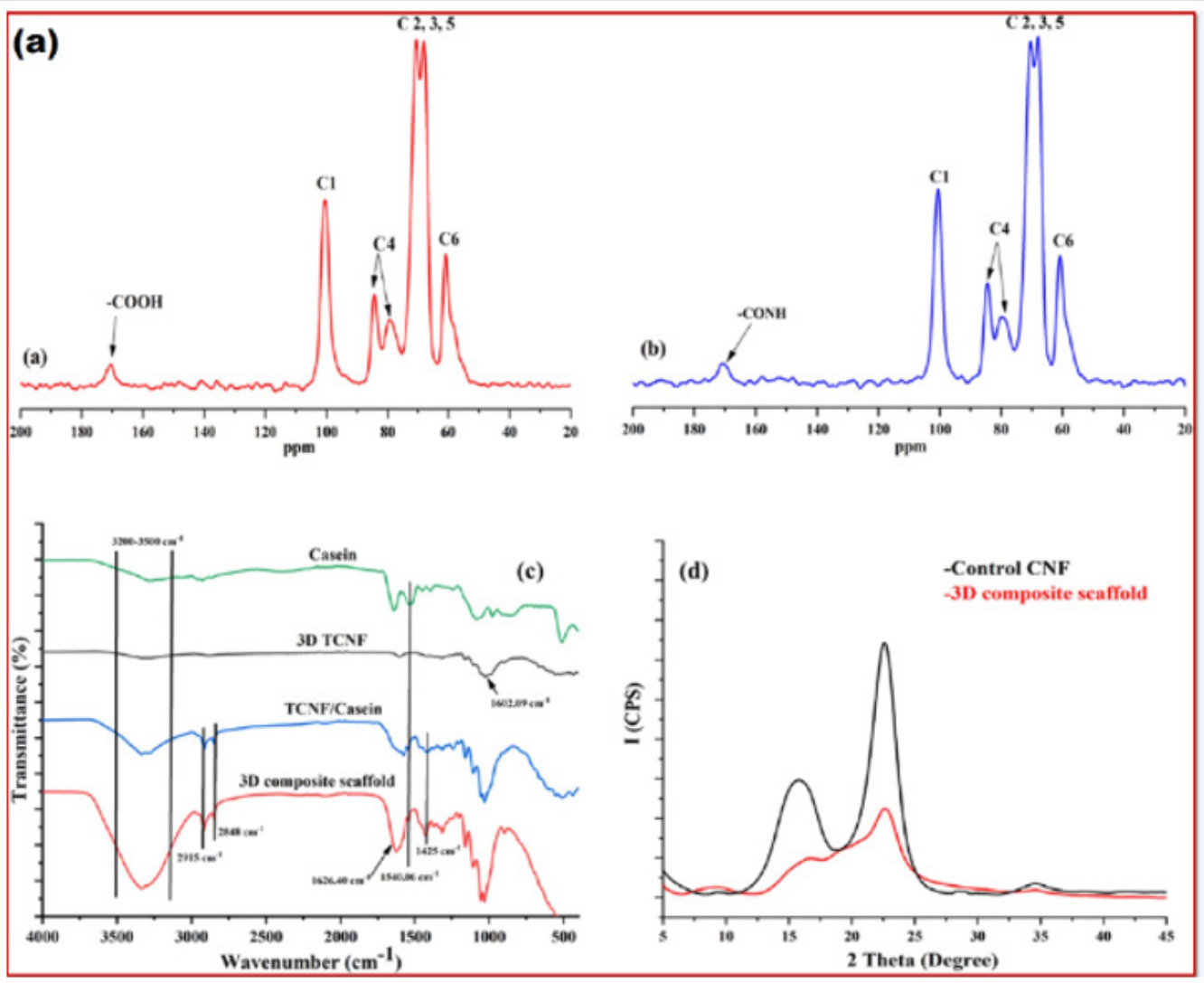

Figure 16: TCNF XPS survey spectra

a) And TCNF@casein conjugate
b) With surface atomic content (%), C 1s high-resolution de-convolution XPS spectra for TCNF
c) And TCNF@casein conjugate
d) O 1s high-resolution deconvolution XPS spectra for TCNF
e) And TCNF@casein conjugate
f) N 1s high-resolution deconvolution XPS spectra for TCNF@casein conjugate
g) SDS-PAGE analysis of bioconjugation between casein and TCNF
h)
i. TCNF,
ii. TCNF@casein mixture without conjugation,
iii. TCNF@casein bioconjugate, and
iv. casein protein were examined through electrophoresis [52].

DOI: 10.26717/BJSTR.2026.64.010038

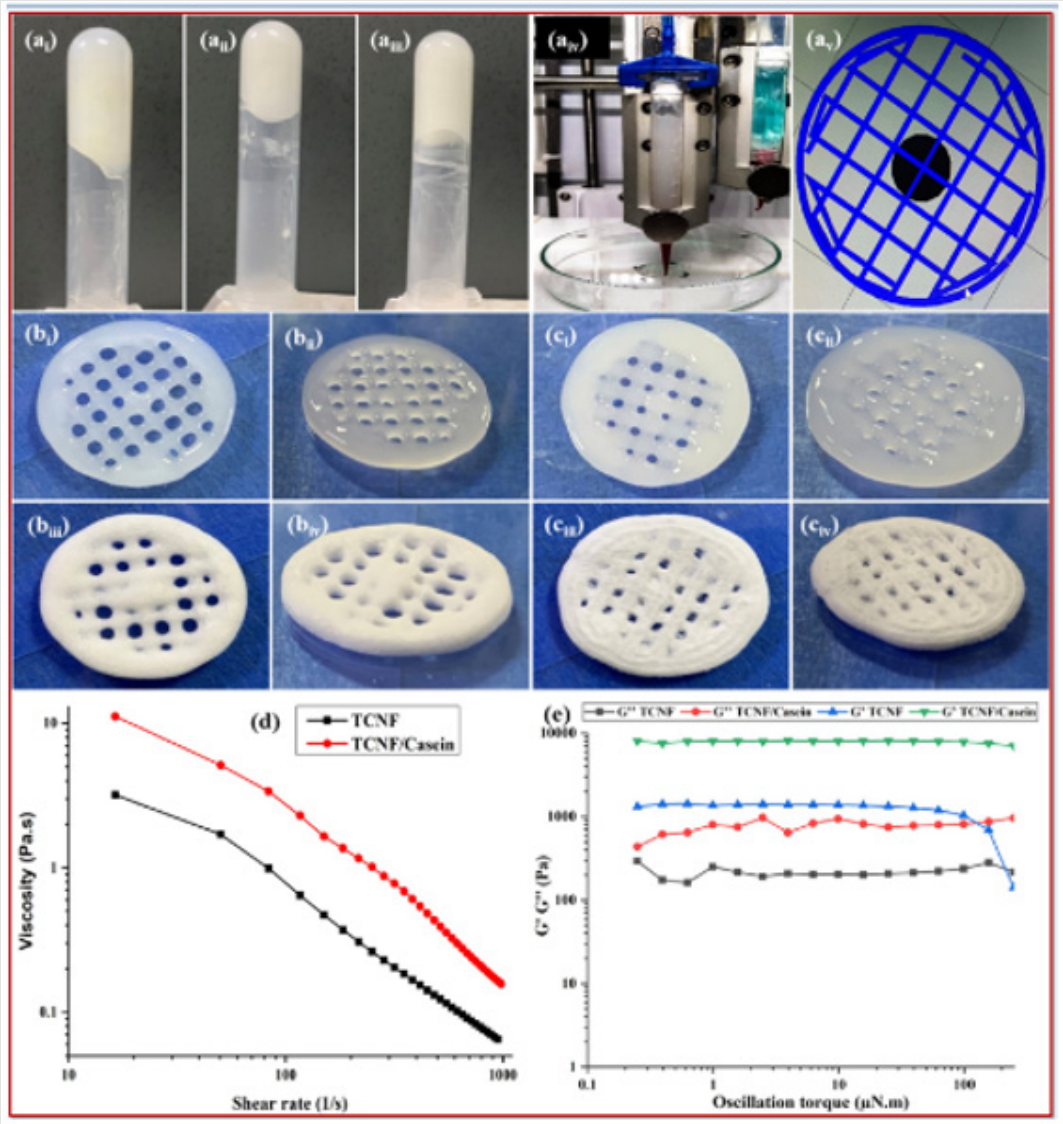

Figure 17: TCNF gel (1.25 wt. %) digitalized images

- (ai), 1.75 wt %
- (aii), and TCNF@casein conjugate (1.75 wt. %)
- (aiii); 3-D printed model and printing procedure
- (aiv−av), 3-D printed TCNF
- ((bi) front view),
- ((bii) side view) and TCNF@casein
- ((biii) front view),
- ((biv) side view); freeze-dried 3-D printed TCNF
- ((ci) front view),
- ((cii) side view) and TCNF/casein after cross-linking with chitosan
- ((ciii) front view),
- ((civ) side view).

Rheological features of the composite bio-inks, shear-thinning features of bioinks (1.75 wt %) at a shear rate ranging from 10 to 1000 s−1 (d), and variation of storage (G′) and loss (G″) moduli of bioinks within an oscillation torque of 0−150 μN m (e) [52].

DOI: 10.26717/BJSTR.2026.64.010038

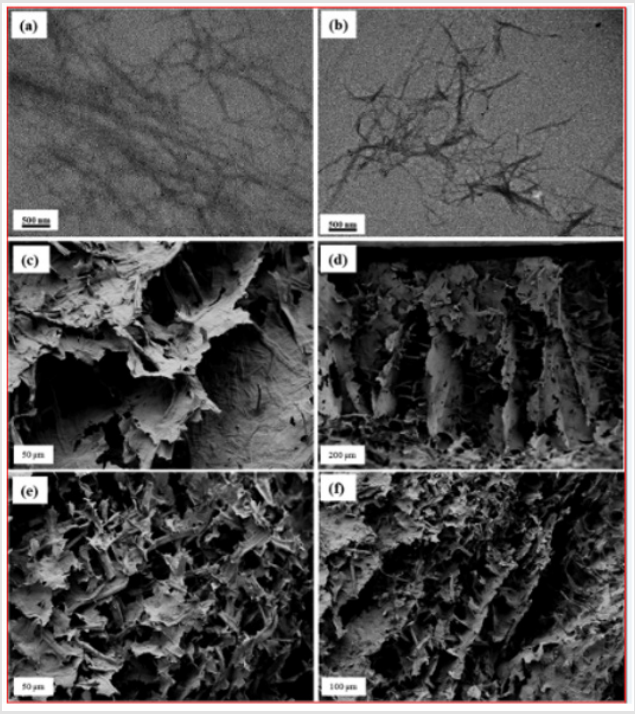

Figure 18: TCNF TEM images
- (a) and bio-conjugated TCNF@casein nanofibrils
- (b); and cross-section SEM images of 3-D TCNF
- (c,d) and 3-D composite scaffold
- (e,f) at differing magnifications [52].

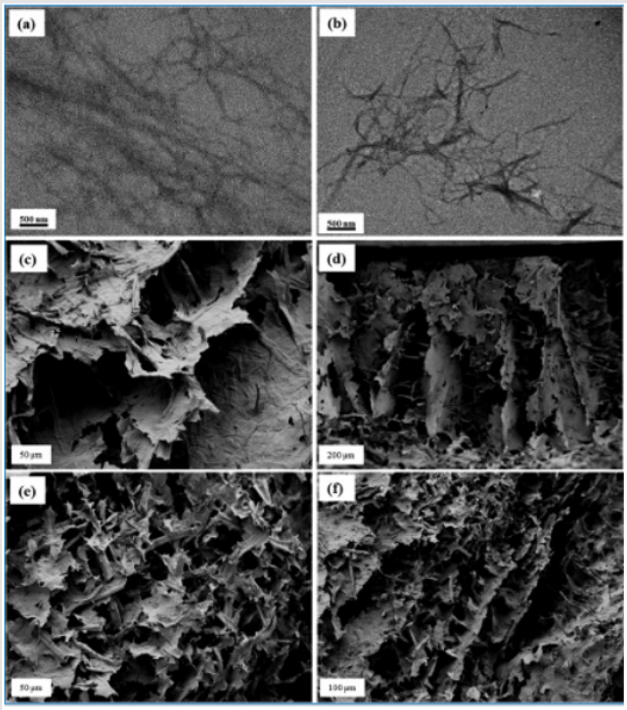

Figure 19: 3-D composite scaffold with RBCs
1. (a–c) SEM images and platelets
2. (d–f) bonded on the surface [52].

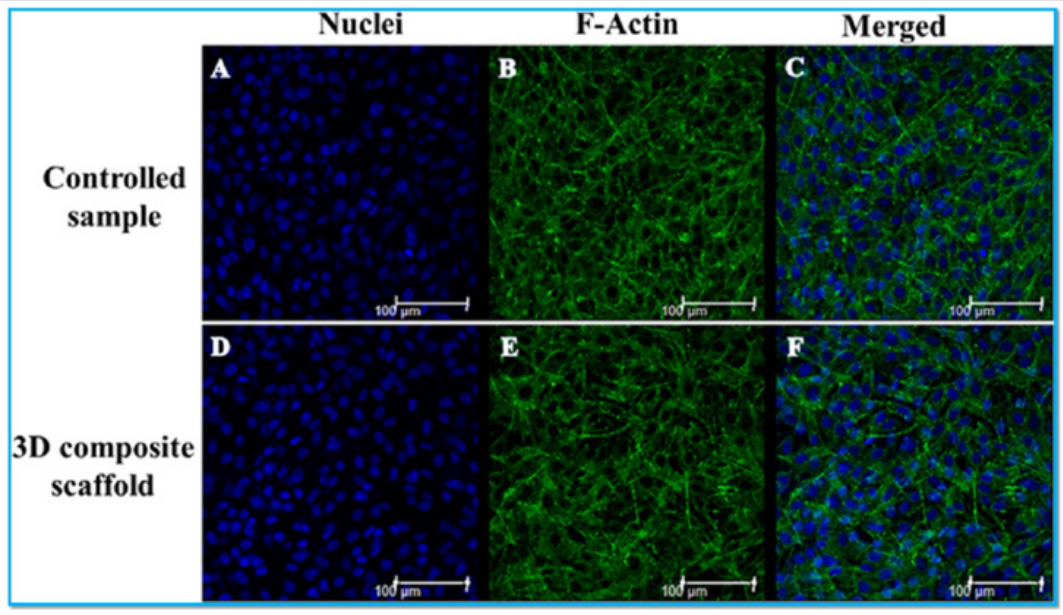

Figure 20: 3-D composite scaffold (D–F) con-focal images of cells and the controlled specimen (A–C) post 72 h of incubation in growth media. The cells cytoskeleton was stained with Actin-Tracker Green 488 (in green), and the nucleus was counterstained with Hoechst 33342 (in blue) [52].

Polymeric Nanoarchitectures for Hemostatic Applications

Nanoarchitectures refer to a multi-phased solid nanomaterial consisting of numerous phases wherein at least one of them has a single dimension in the nanometric range. Differing nanomaterials can be embedded in fabrication of these nanoarchitectures such as nanofibers and nanoparticulates. A vast range of hemostatic entities has been embedded into nanostructures and exhibited elevated hemostatic effectiveness. Some investigations have included nanoparticulates within polymeric matrices. The polymeric-nanoparticulates design improves the interfacial adherence energy, and increment the fracture energy of the hydrogel structure by restraining voids, which enhances the propensity to maintain injuries. In emergency bleeding scenarios, hemostatic materials need rapidly bond and seal the site of bleeding requiring shortening the time of preparation of hemostatic materials, like the time appropriate for in situ injection and time of gelation [52]. It is essential to further enhance the interactivity between the material performance and its practical usage to fabricate the hemostatic materials for emergency usage. In a work, a multifunctional hydrogel with capability of ROS-scavenging features through cross-linking of 2-(hydroxyethyl) methacrylamide (HEMAA), acrylamide (AM), and borax with a greenish tea derivative epigallocatechin-3-gallate (EGCG) was constructed [53].

Further, to hinder bleeding, the scavenged hydrogels accumulated ROS to hinder the cells from ROS-mitigated cell death and proliferation inhibition, thus facilitating wound mending (Figure 21) [53]. In another work, Au NPs were embedded within halloysite nanotubes (HNTs) to garner photo-thermally affiliated impact, wherever the NPs were comingled with chitin for hydrogel preparation [54]. The hydrogel exhibited excellent hemostatic features which effected photo-thermal sterilization, thereby reducing wound afflictions which facilitated fast wound mending (Figure 22) [54]. A study fabricated an intercalated composite, TXA-MTT, situated on montmorillonite (MTT) and tranexamic acid (TXA). The interstitial complexity can low-regulate the mode of the inflammatory parameters IL-1ß, IL-6 and TNF-a and composition of endo-toxin caused by radiation, having prospects for utilization in radiation enteritis and intestinal hemostasis. Though, a water-proof sheet on the dressing surface hindered external surrounding fluid from penetrating the wound with capacity not to absorb or eliminate internal biological fluid [55].

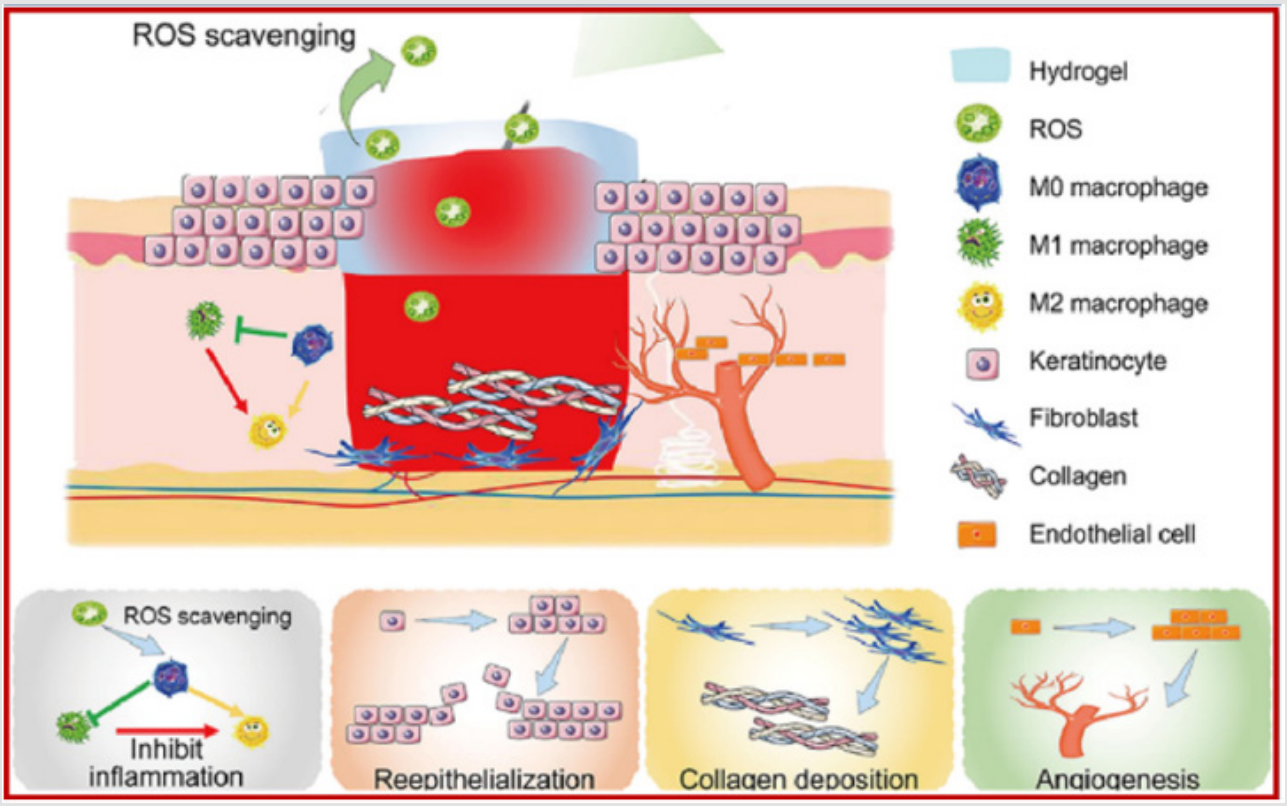

Figure 21: EGCG@PHEMAA@PAM hydrogel scavenged ROS to restrain inflammation and facilitated diabetic wound mending. Reproduced under the terms of the CC BY-NC-ND Creative Commons Attribution 4.0 International License [54]. Copyright 2023, published by Elsevier.

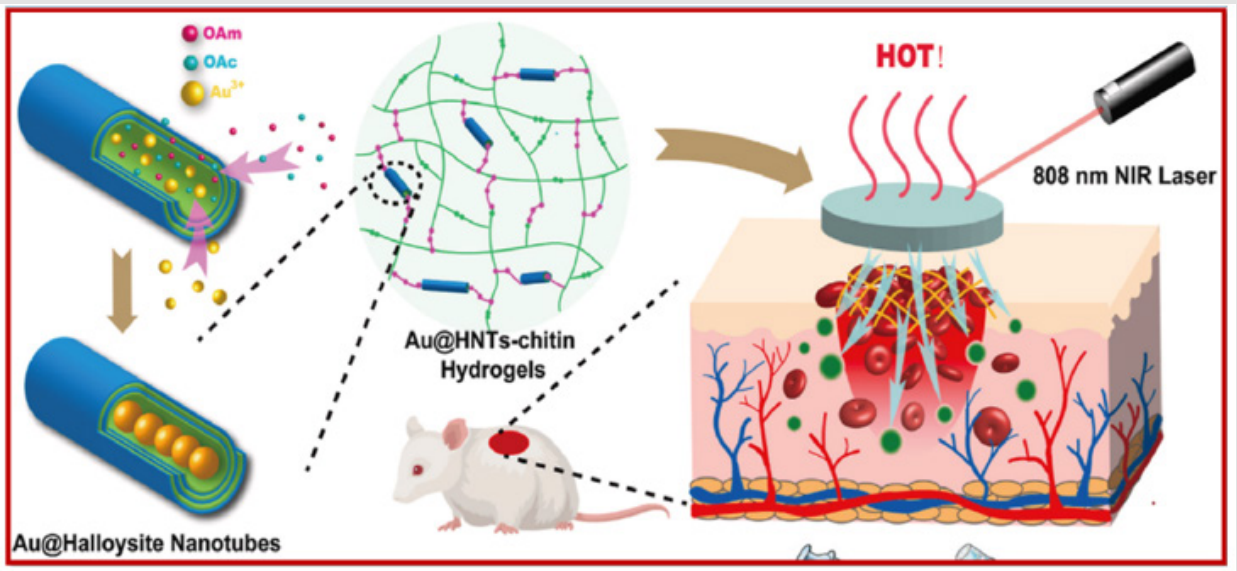

Figure 22: Elucidation of the fabrication procedure of Au@HNTs and photo-thermally affiliated impact of Au@HNTs-chitin hydrogel for attainment of antibacterial and wound mending features. Reproduced under the terms of the CC BY-NC-ND Creative Commons Attribution 4.0 International License. Copyright 2023, published by Elsevier [55].

In an investigation, a biocompatible hyper-long hydroxyapatite (HAP) nanowires/PVA was fabricated as freeze-dried aerogel [56]. The 3D porous aerogel can absorb a large amount of wound exudate thereby preventing thrombus accumulation and excessive inflammation and slowly releasing active Ca^{2+} through HAP; this led to promoting chronic diabetic wound healing in a diabetic mouse model. Another work fabricated a wound dressing through electrospinning of polyurethane for medical gauze garnering a peculiar fluid self-pumping contacting point between the hydrophilic cotton fibers and the hydrophobic nanofibers [57]. Contrastingly to conventional usage of the hydrophobically affiliated sheet in the dressing exterior waterproofing sheet, the hydrophobically inclined sheet in the dressing underwent utilization as a contact sheet on the wound for practical uses [57]. In a bid to facilitate controlling of the wound surrounding during tissue mending, a variety of antibacterial routes have been utilized in hindering bacterial bonding or proliferation, like physical barricades, metal cations/metallic nanoparticulates, cationic polymeric matrices, and so on. Thus, a work fabricated a quaternized chitosan-oxidized sodium alginate hydrogel with β-Ga2O3 nanoparticulates embedded as antibacterial portion [58].

Another investigation utilized a miniature electrospinning device in fabricating CuS composite nanofibers fastly decorated on wounds externally to hinder bleeding, an integrate photo-heat deterioration of hyper bacteria and shorten wound mending duration. In comparison with conventional electrospun fiber mats, the fibers dropped in situ were highly compacted on rough wound surfaces, offering a more rapid hemostasis which was simple in usage during emergency scenarios. Furthermore, methylene blue-included keratin/alginate composite scaffolds was constructed using cryogel route in mediating antibacterial photo-dynamic therapy (aPDT) and produced reactive oxygen species (ROS) to efficiently mitigate drug-resisting pathogens [59]. These drug-enclosed scaffolds underwent highly-bursting releasing wound exudates absorbtion in earlier phase of wound mending thereby further hindering bacterial development to eliminate infection [59]. A work has constructed Ag@CA hydrogel through AgNPs modification with oleic acid and n-butylamine to construct hydrophilic stable colloids [60]. Ag release was hindered via interaction of the hydrogel network/colloids. This construct presented this hydrogel quite different from conventional Ag NPs substrates, which emit the silver ions thereby offering the antibacterial impact [60].

Additionally to enhancement of biocompatible and degradable features of materials, the degree of varying parameters can liably undergo regulation during mending can undergo more regulation to enable the promotion of tissue mending. Hence, another study applied Lycium barbarum polysaccharides in functionalizing montmorillonites (MMT) and deposited it on polyvinyl alcohol hydrogel. The material restrained the secretion of inflammatory parameters, minimized tissue degradation induced by inflammation, minimized feasibility of wound inflammation, and limited the wound repair duration [61]. L-arginine component was embedded within synthetic polyurethane (PU) architecture, a paramount mediator in the wound mending procedure, and regulated the PU structure to inculcate degradability and facilitate gradual releasing of L-arginine to enable promotion of vascularization of the wound tissue (Graphical Abstract) [62].

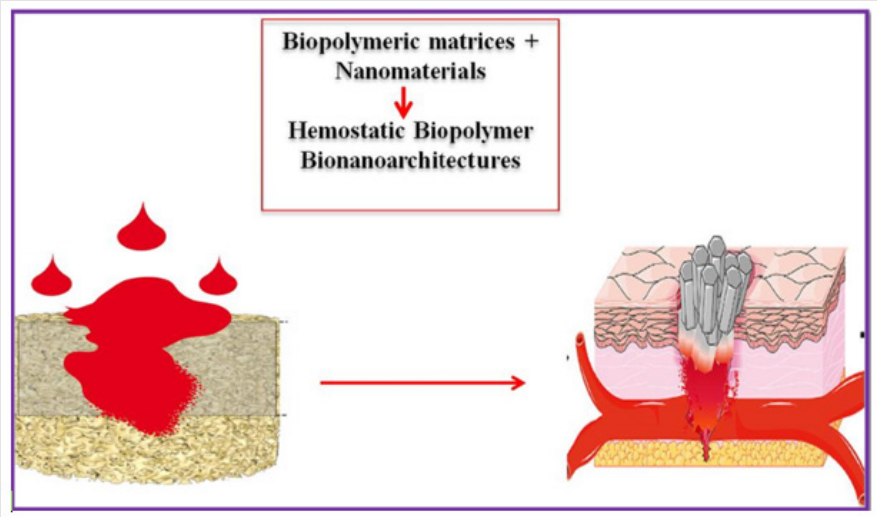

Graphical Abstract.

Another work fabricated a multifunctionalized CS@Ag@TA cryogel, wherein the TA functioned as a cross-linking entity as well as a reducing entity for Ag NPs, while scavenging free radicals to enable wound tissue mending [64]. The porous architecture is another benefit of cryogel, maintaining the material mechanical strength while forming a comfortable micro-surrounding for proliferation of cells [63]. A study constructed a strong polyacrylamide (PAAM)/TA/kaolinite (KA) adhesive hydrogel [64]. Another study embedded silica particulates within poly (lactic-co-glycolic acid) (PLGA) -PEG polymeric sealant to promote tissue adherence. The solution combined with silica underwent spraying directly unto the wound in situ, as the intestinal burst pressure was up to that of cyanoacrylate glue (160 mm Hg) [65].

Challenges and Future Perspectives

Unmitigated bleeding is a notable inducer of traumatic death. Thus, elevatedly efficient hemostats perform a critical function in alleviating hemorrhage and minimizing the degree of death in pre-hospital treatment. Commercially affiliated wound dressings, situated on conventional hemostatic substrates such as fibrin, zeolite and collagen are available on the market. Nevertheless, there are numerous dis-benefits of these products, including infection risks, poor tissue adherence and secondary deterioration. Elevated performing hemostatic substrates are, greatly in quest for alleviating these challenges. Therefore, versatile research with development has undergone production in elevated-performing wound dressings to improve hemostatic effectiveness hence promoting wound repairs. Extensive work is required in mitigating prevalent challenges. Low cost hemostatic substrates are also in great quest. Thus, future investigation of hemostatic substrates may rely on the fabrication of multifunctionalized and cost-efficient hemostatic substrates to satisfy differing clinical enable as elucidated [66].

Chemically treated biopolymeric oriented hemostats with high adherence to tissue will require development for passive hemostasis, devoid of activating the coagulating procedure or inducing systemic thrombosis and embolism. As per clinically translating, surgeons are questing for developing elevated-quality hemostats with fast blood clotting sagacity and simplified usage in any conditions. Hence, researchers in hemostats segment are continuously moved by the quests of surgeons for enhanced device making it easier for in performance of technically challenging surgeries.

Conclusion

Nanotechnological exploration has demonstrated capability of transforming and utilizing the microstructure on a nanometric level, to bequeath nanomaterials exhibiting veritable features including enhanced diffusivity and solubility, ease of penetrating physiologically affiliating barricades, broad specific surfacial area, gradual controlling, and specific releasing of drugs. Asides the chemical constitution of hemostatic materials, other critical parameters includes size, dimension and morphology. Recently, in depth studies has been conducted on nano-hemostatic nanomaterials including nanoparticles, nanosheets, liposomes, and self-assemblage nano-peptides, which offer greater leverage for the development of hemostatic materials. Nanoparticles are colloidal particulates constituting of macromolecular substrates with a solid particulate dimension in range of 10–1000 nm.

Here, charged nanoparticulates are capable of releasing electrostatic effects on blood cells or fibrinogens possessing opposite charges, and neutralize the surfacial charges, initiate its agglomeration, while promoting blood coagulation. A vast range of hemostatic entities has been embedded into nanostructures and exhibited elevated hemostatic effectiveness. Some investigations have included nanoparticulates within polymeric matrices. The polymeric-nanoparticulates design improves the interfacial adherence energy, and increment the fracture energy of the hydrogel structure by restraining voids, which enhances the propensity to maintain injuries. With enlarging scope of nanoparticles and inclusion in biopolymers, a vast range of multifunctional hemostatic bionanoarchitectures with improved features are feasible in future.

Acknowledgement

The Tshwane University of Technology is acknowledged.

Conflict of Interests

Author reports no conflicts.

Funding

Author reports nil funding.

Declarations Statement

The Author declares nothing.

Code or Data Availability

Author declares no software application or custom code.

References

1. Shidhaye Supriya, Priyanka Singanwad, Mayuri Gajghate, Neha Raut, Ruchi Khobragade, et al. (2025) Hemostatic Biopolymers: A Natural Approach for Revolutionizing Blood Loss Control. Polymer Plastics Technology and Materials, p. 1-22.
2. Marimuthu Arumugam, Ravichandran Abimanyu, Khushabu Shekhawat, Ashima Bagaria, Anbalagan M Ballamurugan (2025) Degradable biopolymers for personalized vascular reconstruction: Synthesis, characterization, and animal studies (3191): 1.
3. Hu Xuelian, Sai Li, Yuji Pu, Bin He (2025) Biodegradable Polymeric Microspheres with Enhanced Hemostatic and Antibacterial Properties for Wound Healing. Biomacromolecules 26(2): 1207-1218.
4. Lu Yifan, Xiangxin Lou, Wenxin Wang, Ziting Yang (2025) An Antibacterial Hemostasis Sponge of Gelatin/ε-Poly-L-Lysine Composite. Journal of Biomedical Materials Research Part B: Applied Biomaterials 113(1): e35528.
5. Yu Chunyan, Kai Wang, Shuang Wang, Huihui Zhang, Kehui Qi, et al. (2025) A chitosan/hydroxypropyl methyl cellulose composite sponge with shape memory for rapid hemostasis. New Journal of Chemistry 49(10).

6. Yang Xuekun, Siwei Bi, Changyuan He, Liubo Yuan, Li Zhang, et al. (2025) Rapid Fluid-Induced-Expanding Chitosan-Derived Hemostatic Sponges with Excellent Antimicrobial and Antioxidant Properties for Incompressible Hemorrhage and Wound Healing. Biomacromolecules 6(1): 689-704.
7. Mrozińska Zdzisława, Małgorzata Świerczyńska, Michał Juszczak, Katarzyna Woźniak, Marcin H Kudzin, et al. (2025) Evaluation of Antimicrobial Activity, Hemostatic Efficacy, Blood Coagulation Dynamics, and DNA Damage of Linen–Copper Composite Materials. Journal of Composites Science 9(1): 30.
8. Zeng Xingling, Zhaohui Sun, Lidan Chen, Xiaoxia Zhang, Xin Guo, et al. (2025) Co-assembled biomimetic fibrils from collagen and chitosan for performance-enhancing hemostatic dressing. Biomaterials Science 13(1): 236-249.
9. Zeng Xingling, Zhaohui Sun, Lidan Chen, Xiaoxia Zhang, Xin Guo, et al. (2025) Co-assembled biomimetic fibrils from collagen and chitosan for performance-enhancing hemostatic dressing. Biomaterials Science 13(1): 236-249.
10. He Wei, Jinxiu Liu, Zhongjia Liu, Yan Chen, Huixuan Gan, et al. (2025) Protoporphyrin IX-modified chitosan/sodium alginate based cryogels for rapid hemostasis and antibacterial photodynamic therapy of infected wound healing. International Journal of Biological Macromolecules 303: 140614.
11. Farasati Far Bahareh, Leila Jameie, Parsa Taromi, Reza Nahavndi, Edris Jamshidi (2025) Dermal and Oral Wound Healing. In Green Biomaterials in Tissue Engineering. American Chemical Society, pp. 297-329.
12. Sukhodub Leonid, Oleksii Korenkov, Liudmyla Sukhodub, Mariia Kumeda (2025) Regenerative Potential of Biopolymers-Calcium Phosphate Osteogenic Composites in the Healing of an Experimental Defect of the Parietal Bone. Biomaterials and Biosystems 18: 100112.
13. Ding Ruochen, Zhan Shu, Jian Yang, Ren Chen (2025) Selectively oxidized chitin as a degradable and biocompatible hemostat for uncontrolled bleeding and wound healing. International Journal of Biological Macromolecules 304: 140906.
14. Sheergujri Danish Ahmad, Murtaza Ahmad Khanday, Aisha Noor, Mohd Adnan, Iqra Arif, et al. (2025) Biopolymer Gels as Smart Drug Delivery and Theranostic Systems. Journal of Materials Chemistry B.
15. Abedi Mehdi, Mostafa Arbabi, Razieh Gholampour, Javid Amini, Zahra Barandeh, et al. (2025) Zinc oxide nanoparticle-embedded tannic acid/chitosan-based sponge: A highly absorbent hemostatic agent with enhanced antimicrobial activity. International Journal of Biological Macromolecules 300: 140337.
16. Tran Ngoc Phan, Yoko Okahisa, Satoko Okubayashi (2025) Chitosan aerogel containing mechanically fibrillated fibroin and its model test for wound dressing. Polymer Engineering & Science 65(3): 1340-1349.
17. Jahan Nusrat, Md Abdullah Al Fahad, Prayas Chakma Shanto, Hyeyoung Kim, Byong Taek Lee, et al. (2025) Development of self-gelling powder combining chitosan/bentonite nanoclay/sodium polyacrylate for rapid hemostasis: *In vitro* and *in vivo* study. International Journal of Biological Macromolecules 291: 139123.
18. Anh Tin Tran, Thong Lam Vu, Khoi Minh Le, My-An Tran Le, Kieu Thi Thuy Nguyen, et al. (2025) Fabrication and characterization of hydrophobic montmorillonite-modified PCL/COS nanofibrous electrospun membrane for hemostatic dressing. Colloids and Surfaces a Physicochemical and Engineering Aspects 708: 135975.
19. Kogje Mithilesh, Ajinkya Satdive, Siddhesh Mestry, Mhaske T (2025) Biopolymers: a comprehensive review of sustainability, environmental impact, and lifecycle analysis. Iranian Polymer Journal 34(9): 1-44.
20. Hou Xueyan, Yalin Guan, Yanan Lu, Yuxin Wang, Suyue Xu, et al. (2025) Chitosan-based thermosensitive injectable hydrogel with hemostatic and antibacterial activity for preventing breast cancer postoperative recurrence and metastasis via chemo-photothermal therapy. International Journal of Biological Macromolecules 290: 138930.
21. Feraru Alexandra, Zsejke Réka Tóth, Klára Magyari, Monica Baia, Tamás Gyulavári, et al. (2025) The effect of nanoceria on the alginate gum arabic cross-linking mechanism and *in vitro* behavior as a wound dressing. International Journal of Biological Macromolecules 288: 138569.
22. Wu Z, Dongdong Lu, Shuo Sun, Manqi Cai, Lin Lin, et al. (2025) Material Design, Fabrication Strategies, and the Development of Multifunctional Hydrogel Composites Dressings for Skin Wound Management. Biomacromolecules 26(3): 1419-1460.
23. Zhao Kaixiong, Kangsi Zhou, Xu Chang, Shuming Liu, Weizhao Hu, et al. (2025) Harnessing Nanoconfinement-Enhanced Hydrogen Bonding and Multi-Scale Structures for High-Performance Sustainable Foam Materials. Composites Part B Engineering 297(31): 112318.
24. Kurtuluş OÇ, Ondaral S, Emin N Kadak AE (2025) Bioaerogels produced from tempo oxidized nano cellulose with chitosan, gelatin, and alginate: general performances for wound dressing application. Cellulose 32(1): 295-311.
25. Li Yang, Yinfeng Tan, Huange Zhao, Shiting Chen, Azadeh Nilghaz, et al. (2025) Green biosynthetic silver nanoparticles from Ageratum conyzoides as multifunctional hemostatic agents: Combining hemostasis, antibacterial, and anti-inflammatory properties for effective wound healing. Materials Today Bio 31: 101468.
26. Wei Yanxing, Qiwei Yu, Yuxi Zhan, Hao Wu, Qiang Sun (2025) Piezoelectric hydrogels for accelerating healing of diverse wound types. Biomaterials Science 16: 100137.
27. Mohamed E, Fitzgerald A, Tsuzuki T (2021) The role of nanoscale structures in the development of topical hemostatic agents. Materials Today Nano 16: 100137.
28. Gobi R, Babu RS (2025) *In-vitro* investigation of chitosan/polyvinyl alcohol/TiO_2 composite membranes for wound regeneration. Biochemical and Biophysical Research Communications 742: 151129.
29. Liu Yuqing, Wen Zhong, Yongfeng Ai, Malcolm Xing (2025) Double Cross-linked Methacrylated Carboxymethyl Pea Starch Cryogels with Highly Compressive Elasticity and Hemostatic Function. Biomacromolecules 26(2): 883-899.
30. Nikhil K, Shaji S (2025) Polymer Blends and Composites-Biomedical Application. In Smart Ways of Biomaterial Designing Synthesis and Characterization (pp. 99-121). CRC Press.
31. Dutta J, Devi N (2021) Preparation, optimization, and characterization of chitosan-sepiolite nanocomposite films for wound healing. International Journal of Biological Macromolecules 186: 244-254.
32. Patel S, Srivastava S, Singh MJ, Singh D (2018) Preparation and optimization of chitosan-gelatin films for sustained delivery of lupeol for wound healing. International Journal of Biological Macromolecules 107: 1888-1897.
33. Ambrogi V, Pietrella D, Nocchetti M, Casagrande S, Moretti V, et al. (2017) Montmorillonite–chitosan–chlorhexidine composite films with antibiofilm activity and improved cytotoxicity for wound dressing. Journal of Colloid and Interface Science 491: 265-272.
34. Wang X, Mu B, Zhang H, Du Y, yang F, et al. (2023) Incorporation of mixed-dimensional palygorskite clay into chitosan/polyvinylpyrrolidone nanocomposite films for enhancing hemostatic activity. International Journal of Biological Macromolecules 237: 124213.
35. Li X, Li C, Chen M, Shi Q, Sun R, et al. (2018) Chitosan/rectorite nanocomposite with injectable functionality for skin hemostasis. Journal of Materials Chemistry 6(41): 6544-6549.

36. Yang Y, Wang X, Li Y, Yang F, Liu X, et al. (2024) Dencichine/palygorskite nanocomposite incorporated chitosan/polyvinylpyrrolidone film for accelerating wound hemostasis. International Journal of Biological Macromolecules 275: 133399.

37. Arshad MS, Qaiser M, Mahmood K, Shoaib MH, Ameer N, et al. (2022) Chitosan/halloysite nanotubes microcomposites: A double header approach for sustained release of ciprofloxacin and its hemostatic effects. International Journal of Biological Macromolecules 212: 314-323.

38. Mahbub MSI, Bae SH, Gwon JG, Lee BT (2023) Decellularized liver extracellular matrix and thrombin loaded biodegradable TOCN/Chitosan nanocomposite for hemostasis and wound healing in rat liver hemorrhage model. International Journal of Biological Macromolecules 225: 1529-1542.

39. Mahbub MI, Bae SH, Gwon JG, Lee BT (2023) Decellularized liver extracellular matrix and thrombin loaded biodegradable TOCN/Chitosan nanocomposite for hemostasis and wound healing in rat liver hemorrhage model. International Journal of Biological Macromolecules 225: 1529-1542.

40. Zhu X, Wang J, Wu S, Liu T, Lin G, et al. (2022) Biological application of novel biodegradable cellulose composite as a hemostatic material. Hindawi Mediators of Inflammation 2022: 4083477.

41. Wu Zeyong, Yucang Shi, Bing Zhang, Hongwei Liu, Peihua Zhang (2025) Jellyfish Collagen Grafted with Hydroxybutyl Chitosan and Protocatechuic Acid Adhesive Sponge with Antibacterial Activity for Rapid Hemostasis. ACS omega 10(3): 2986-2995.

42. Wang Wenxin, Haochen Yao, Jie Xia, Xinjian Wan, Jinglei Wu (2025) Chitosan-based immunomodulatory bioadhesive hydrogel promotes liver hemostasis and repair. Carbohydrate Polymers 353: 123268.

43. Wang Y, Zhao Y, Qiao L, Zou F, Xie Y, et al. (2021) Cellulose fibers-reinforced self-expanding porous composite with multiple hemostatic efficacy and shape adaptability for uncontrollable massive hemorrhage treatment. Bioactive Materials 6(7): 2089-2104.

44. Rao Kummara Madhusudana, Mooni Siva Prasad, Anam Giridhar Babu, P Rosaiah, Mohammad Rezaul Karim, et al. (2025) Tissue adhesive hyaluronan-quercetin (Ago)@ halloysite-fungal carboxymethyl chitosan nanocomposite hydrogels for wound dressing applications. International Journal of Biological Macromolecules 284: 137849.

45. Rao Kummara Madhusudana, Mooni Siva Prasad, Anam Giridhar Babu, P Rosaiah, Mohammad Rezaul Karim, et al. (2025) Tissue adhesive hyaluronan-quercetin (Ago)@ halloysite-fungal carboxymethyl chitosan nanocomposite hydrogels for wound dressing applications. International Journal of Biological Macromolecules 284: 137849.

46. Chen Nuoya, Derong He, Xin Tan, Liqin Ge (2025) A metal-polyphenol microcapsule functionalized hydrogel for effective hemostasis. Colloids and Surfaces A Physicochemical and Engineering Aspects 707: 135830.

47. Chen Nuoya, Derong He, Xin Tan, Liqin Ge (2025) A metal-polyphenol microcapsule functionalized hydrogel for effective hemostasis. Colloids and Surfaces A Physicochemical and Engineering Aspects 707: 135830.

48. Rao Kummara Madhusudana, Mooni Siva Prasad, Anam Giridhar Babu, P Rosaiah, Mohammad Rezaul Karim, et al. (2025) Tissue adhesive hyaluronan-quercetin (Ago)@ halloysite-fungal carboxymethyl chitosan nanocomposite hydrogels for wound dressing applications. International Journal of Biological Macromolecules 284: 137849.

49. Yao Cheng Jung, Shu Jyuan Yang, Ming Jium Shieh, Tai Horng Young (2025) Development of a Chitosan-Silver Nanocomposite/β-1, 3-Glucan/Hyaluronic Acid Composite as an Antimicrobial System for Wound Healing. Polymers 17(3): 350.

50. Cui Y, Huang Z, Lei L, Li Q, Jiang J, et al. (2025) Robust hemostatic bandages based on nanoclay electrospun membranes. Nature Communications 12: 5922.

51. Biranje S, Sun J, Cheng L, Cheng Y, Shi Y, et al. (2022) Development of Cellulose Nanofibril/Casein-Based 3D Composite Hemostasis Scaffold for Potential Wound-Healing Application. ACS Appl Mater Interfaces 14(3): 3792-3808.

52. Ianev Daiana, Barbara Vigani, Caterina Valentino, Milena Sorrenti, Laura Catenacci, et al. (2025) Whey protein-chitosans complexes as sustainable and value-added biomaterials for wound healing. Carbohydrate Polymer Technologies and Applications 9: 100643.

53. G Jia, Z Li, H Le, Z Jiang, Y Sun, et al. (2023) Green tea derivative-based hydrogel with ROS-scavenging property for accelerating diabetic wound healing. Mater Des 225: 111452.

54. Zhao P, Feng Y, Zhou Y, Tan C, Liu M (2023) Gold@Halloysite nanotubes-chitin composite hydrogel with antibacterial and hemostatic activity for wound healing. Bioact Mater 20: 355-367.

55. F Ma, S Sui, Z Yang, T Ye, L Yang, et al. (2022) Evaluation of novel tranexamic acid/montmorillonites intercalation composite, as a new type of hemostatic material. BioMed Res Int.

56. Y Zheng, W Ma, Z Yang, H Zhang, J Ma, et al. (2022) An ultralong hydroxyapatite nanowire aerogel for rapid hemostasis and wound healing. Chem Eng J 430: 132912.

57. L Shi, X Liu, W Wang, L Jiang, S Wang (2019) A self-pumping dressing for draining excessive biofluid around wounds. Adv Mater 31(5): e1804187.

58. Negi D, Singh Y (2023) Gallium oxide nanoparticle-loaded, quaternized chitosan-oxidized sodium alginate hydrogels for treatment of bacteria-infected wounds. ACS Appl Nano Mater 6: 14.

59. Liu F, Zhang J, Liu J, Zhou Q, Liu Z, et al. (2020) Bifunctional CuS composite nanofibers via in situ electrospinning for outdoor rapid hemostasis and simultaneous ablating superbug. Chem Eng J 401: 126096.

60. Xu M, Ji X, Huo J, Chen J, Liu N, et al. (2023) Non releasing AgNP colloids composite hydrogel with potent hemostatic, photodynamic bactericidal and wound healing-promoting properties. ACS Appl Mater Interfaces 15(14): 17742-17756.

61. Shi S, Lan X, Feng J, Ni Y, Zhu M, et al. (2022) Hydrogel loading 2D montmorillonite exfoliated by anti-inflammatory Lycium barbarum L. polysaccharides for advanced wound dressing. Int J Biol Macromol 209: 50-58.

62. Zou F, Wang Y, Zheng Y, Xie Y, Zhang H, et al. (2022) A novel bioactive polyurethane with controlled degradation and L-Arg release used as strong adhesive tissue patch for hemostasis and promoting wound healing. Bioact Mater 17: 471-487.

63. Xu G, Xu N, Ren T, Chen C, Li J, et al. (2022) Multifunctional chitosan/silver/tannic acid cryogels for hemostasis and wound healing. Int J Biol Macromol 208: 760-771.

64. X Fan, S Wang, Y Fang, P Li, W Zhou, et al. (2020) Tough polyacrylamide-tannic acid-kaolin adhesive hydrogels for quick hemostatic application. Mater Sci Eng C 109: 110649.

65. J L Daristotle, S T Zaki, L W Lau, L Torres Jr, A Zografos, et al. (2019) Improving the adhesion, flexibility, and hemostatic efficacy of a sprayable polymer blend surgical sealant by incorporating silica particles. Acta Biomater 90: 205-216.

66. Feng C, Lu W, Liu Y, Liu H, Chen Y, et al. (2022) A hemostatic keratin/alginate hydrogel scaffold with methylene blue mediated antimicrobial photodynamic therapy. J Mater Chem B 10(25): 4878-4888.

ISSN: 2574-1241

DOI: 10.26717/BJSTR.2026.64.010038

Christopher Igwe Idumah. Biomed J Sci & Tech Res

Submission Link: https://biomedres.us/submit-manuscript.php